ASTRONOMY & ASTROPHYSICS
SUPPLEMENT SERIES

Astron. Astrophys. Suppl. Ser. **105,** 91-113 (1994)

High resolution radio observations of intermediate redshift quasars and radio galaxies

W.J. Bogers[1], R. Hes[1], P.D. Barthel[1] and J.A. Zensus[2]

[1] Kapteyn Astronomical Institute, P.O.Box 800, NL-9700 AV Groningen, The Netherlands
[2] National Radio Astronomy Observatory, P.O.Box 0, Socorro, NM 87801, U.S.A.

Received October 18; accepted November 24, 1993

Abstract. — We present radio maps of a collection of intermediate redshift quasars and radio galaxies mostly taken from the 3C and 4C catalogues. The sources were observed with the Very Large Array (VLA) at one or more of the following frequencies: 15 GHz, 8.4 GHz or 1.4 GHz. Several basic source parameters are given, and new results on individual sources are briefly discussed. Among these results are first-time detections of radio jets in quasars and novel detections of cores in radio galaxies.

Key words: radio continuum: galaxies — galaxies: active — quasars: general

1. Introduction

Extragalactic radio sources provide a unique opportunity to study the conditions in the early universe and to determine how these conditions have evolved with time. Measurements of the morphology of distant quasars indicate that sources at large look-back times reside in a much denser environment than low redshift sources (e.g. Barthel & Miley 1988). This topic is still strongly debated however (Kapahi 1990), and a larger body of high resolution radio maps of quasars and radio galaxies is clearly needed. Some substantial data sets on quasars have been published recently, of which we mention here Price et al. (1993) and Lonsdale et al. (1993) on low and high redshift quasars respectively. Less satisfactory is the number of published high quality maps of radio galaxies. There is an increasing need for such data in order to make comparative studies of radio galaxy and quasar properties and evolution, in particular in the context of the widely discussed unified models of these classes (Antonucci 1993). High resolution radio maps of 41 quasars and radio galaxies are presented here, which will be useful for this purpose.

The observations discussed in this paper have been taken for the above mentioned programmes. The first programme is concerned with the cosmological evolution of size and shape of radio sources. One subsample used in that study and of which the radio maps are presented here consists of radio-loud quasars with redshifts in the range $0.5 < z < 0.7$. These were selected from the Hewitt & Burbidge (1987) catalogue as having steep spectra at centimeter wavelengths ($\alpha \geq 0.6, S_\nu \propto \nu^{-\alpha}$) and having luminosities at 5 GHz in excess of 26.0 W Hz^{-1}. Most of the sample quasars appear in the 3C and 4C catalogues. For further details on this project we refer to Bogers et al. (1994).

The second programme aims at testing predictions of the unified models of powerful radio galaxies and quasars (e.g. Barthel 1989; Hes et al. 1993). For the necessary synthesis of optical and radio data we have observed a number of sources from the 3C catalogue (Spinrad et al. 1985) in the $0.2 < z < 0.9$ range with no, or incomplete, radio data in the literature. These sources are all steep-spectrum objects, and include both radio galaxies and quasars.

In Sect. 2 the observations and subsequent data reduction in both programmes are described, while Sect. 3 discusses the individual objects. The results are presented as an atlas of radio images of quasars and powerful radio galaxies in the $0.2 < z < 0.9$ redshift interval. Tables 1 through 3 contain the observational parameters, Tables 4 through 6 the map parameters, and Tables 7 and 8 summarize several basic source parameters measured from the radio maps. In Table 9 the (B1950) radio positions of the newly detected cores are given, together with their fluxes.

2. Observations and data reduction

The observations of the quasars in the first programme were carried out on January 10-11, 1987 with the VLA in C configuration. The observing frequency was 15 GHz (2 cm). Two snapshots of typically ten minutes each at dif-

Send offprint requests to: R. Hes or P.D. Barthel

ferent hour angles were made to increase the UV coverage. The typical beamsize in the final maps is 1.3″ (Table 1).

For the second programme we have observed radio galaxies and quasars at redshifts $0.2 < z < 0.9$ from the 3C catalogue. These data are at two frequencies. Observations at frequency 8.4 GHz (3.6 cm) were performed with the VLA in B array (December 1991) or A array (December 1992), leading to beamsizes of approximately 0.7″ and 0.2″, respectively (Table 2). Additional observations at frequency 1.4 GHz (20 cm) with the VLA in A array were taken in December 1991, yielding a beamsize of about 1.2″ (Table 3). All integrations consist of two snapshots of typically twenty minutes each, taken with the source at different hour angles. This strategy has been followed to increase the UV coverage, especially since most of these sources are near the equator.

The radio data were of high quality, and there was no need for extensive flagging of discrepant points. Reduction of the data was performed using standard NRAO AIPS image processing routines, including several steps of self-calibration (phase only, followed by amplitude self-calibration). Several successive self-calibration and cleaning cycles generally led to a rapid convergence towards the maps presented here.

3. Results

The contour maps are displayed in Figs. 1 to 52. Contours are multiples of the rms noise level in the radio images (see Tables 4, 5 and 6). Top contours represent 95% of the peak flux. Crosses denote the (B1950) position of the optical object, as given in Tables 1, 2 and 3. Positions quoted throughout this paper all refer to epoch B1950. All optical positions in Table 1 were taken from the NASA/IPAC extragalactic database (NED), while the positions for all objects in Tables 2 and 3, except 1508+080 (3C313), were taken from the 3C listing (Spinrad et al. 1985 and recent updates). The position of 1508 + 080 (3C313) was taken from Baum et al. (1988). Below we will briefly discuss each object, giving references to the literature where additional radio maps can be found.

Tables 7 and 8 list measured source parameters: flux densities, largest angular sizes, linear sizes and position angles on the sky. The largest angular sizes (denoted by LAS) are measured between the outermost peaks in the radio brightness distribution of the sources. The position angles measured for the sources are those of the line connecting the peaks. For the extended sources the peaks are in most cases the hot spots in the lobes. The angular size given for the few compact quasars, is the FWHM of a deconvolved 2-D Gaussian fit to the brightness distribution. In order to calculate linear sizes (denoted by LIN) we have assumed a Hubble constant of $H_0 = 75\,\mathrm{km\,s^{-1}\,Mpc^{-1}}$ and a deceleration parameter of $q_0 = \frac{1}{2}$.

Tabulated flux densities were measured from the radio images by placing appropriate boxes around the emission regions. Comparison with the White & Becker (1992) 1.4 GHz single dish flux densities, indicates deficits in the range 5% to 15%, with the exception of 0528 + 064 (3C 142.1) and 0742+021 (3C 187), which have deficits of 25%. These deficits are presumably due to low surface brightness steep-spectrum lobe emission, to which the VLA in the present set-up is insensitive.

3.1. *Notes on individual objects*

0035+130 *(3C 16, Fig. 1)* The 5 GHz image of this galaxy of Jenkins et al. (1977) revealed only the southern component of this double source. The faint northern radio component appeared clearly in a combined VLA A and B array 1.4 GHz (Leahy & Perley 1991). This structure is also found in our 1.4 GHz map. The double source has a size of 78″ and appears strongly asymmetric, with the southern component being much more luminous than the northern. No radio core has been detected and the optical counterpart lies in the middle of the southern radio lobe.

0115+027 *(3C 37, Fig. 2)* Hintzen et al. (1983) give a 1.4 GHz VLA A array map of this quasar, in which more diffuse emission is detected than in our 15 GHz image. In Saikia et al. (1989) a 4.8 GHz VLA B array map can be found. Notable in this object is the low surface brightness emission between core and outer extremities, masking the presence of a possible jet.

0128+061 *(3C 44, Fig. 3)* We could not locate radio data of this galaxy in the literature. Our 8.4 GHz map at 0.8″ resolution shows a fairly large (LAS=65″) double, with well defined hotspots in both lobes. We can not unambiguously identify the core of this radio galaxy since it is confused with extended emission.

0155−109 *(PKS, Fig. 4)* No radio images of this quasar were found in the literature. Two components, separated by 4.3″, can be distinguished: a very bright component of which the position of the peak coincides with the optical quasar position, and a much weaker component to the southeast of this.

0159−117 *(3C 57, Fig. 5)* The southeastern component which we observe in the 15 GHz image of this quasar is not present in the 1.4 GHz VLA A array map of Hintzen et al. (1983). The 8.4 GHz VLA A array map given by Price et al. (1993) does show this component, and furthermore resolves the main component into two subcomponents, separated by 2″.

0222−008 *(4C−00.12, Fig. 6)* Radio maps of this quasar can be found in Downes et al. (1986), who show a 1.5 GHz VLA A array image, and in Hintzen et al. (1983), who give a 1.4 GHz VLA A array image. Both maps show excellent agreement with our 15 GHz map.

Table 1. 15 GHz observations (C array) – observational parameters

(1)	(2)	(3)	(4)	(5)	(6)	(7)	(8)	(9)
Source	Alt. name	Type	z	RA (h m s)	DEC (° ′ ″)	VLA conf.	Beam (″, °)	Epoch
0115 + 027	3C37	Q	0.672	01:15:43.64	+02:42:19.8	C, 15 GHz	1.47 x 1.34, 2	1/87
0155 − 109	PKS	Q	0.616	01:55:14.06	−10:58:16.6	C, 15 GHz	1.77 x 1.30, −2	1/87
0159 − 117	3C57	Q	0.669	01:59:30.36	−11:46:59.7	C, 15 GHz	1.79 x 1.27, 1	1/87
0222 − 008	4C−00.12	Q	0.687	02:22:34.63	−00:49:03.4	C, 15 GHz	1.52 x 1.36, 7	1/87
0349 − 146	3C95	Q	0.614	03:49:09.46	−14:38:05.4	C, 15 GHz	1.81 x 1.24, −9	1/87
0538 + 498	3C147	Q	0.545	05:38:43.55	+49:49:42.8	C, 15 GHz	1.23 x 1.13, 30	1/87
0610 + 260	3C154	Q	0.580	06:10:43.75	+26:05:30.0	C, 15 GHz	1.29 x 1.26, 26	1/87
0704 + 384	4C38.20	Q	0.579	07:04:08.39	+38:26:57.3	C, 15 GHz	1.22 x 1.21, 44	1/87
0906 + 430	3C216	Q	0.670	09:06:17.28	+43:05:59.0	C, 15 GHz	1.53 x 1.24, 75	1/87
0932 + 022	4C02.27	Q	0.659	09:32:42.93	+02:17:39.6	C, 15 GHz	1.94 x 1.84, −49	1/87
0937 + 391	4C39.27	Q	0.618	09:37:59.10	+39:07:31.0	C, 15 GHz	1.58 x 1.25, 86	1/87
1132 + 303	3C261	Q	0.614	11:32:16.25	+30:22:02.3	C, 15 GHz	1.63 x 1.28, −82	1/87
1136 − 135	PKS	Q	0.554	11:36:38.51	−13:34:05.9	C, 15 GHz	1.56 x 1.28, −31	1/87
1137 + 660	3C263	Q	0.652	11:37:09.34	+66:04:26.9	C, 15 GHz	1.74 x 1.33, 61	1/87
1150 + 094	4C09.39	Q	0.698	11:50:38.41	+09:30:44.3	C, 15 GHz	1.68 x 1.60, −50	1/87
1156 + 631	4C63.15	Q	0.594	11:56:04.65	+63:11:09.7	C, 15 GHz	1.75 x 1.33, 61	1/87
1241 + 166	3C275.1	Q	0.557	12:41:27.58	+16:39:18.0	C, 15 GHz	1.91 x 1.54, −60	1/87
1305 + 069	3C281	Q	0.599	13:05:22.48	+06:58:12.9	C, 15 GHz	1.43 x 1.35, −32	1/87
1327 − 214	PKS	Q	0.528	13:27:23.36	−21:26:33.8	C, 15 GHz	1.64 x 1.22, −28	1/87
1335 − 061	4C−06.35	Q	0.625	13:35:31.20	−06:11:56.7	C, 15 GHz	1.56 x 1.33, −29	1/87
1423 + 242	4C24.31	Q	0.649	14:23:34.67	+24:17:32.1	C, 15 GHz	1.39 x 1.31, −89	1/87
1451 + 097	4C09.52	Q	0.627	14:51:27.90	+09:46:33.0	C, 15 GHz	1.54 x 1.46, −57	1/87
1618 + 177	3C334	Q	0.555	16:18:07.31	+17:43:30.4	C, 15 GHz	1.52 x 1.36, −67	1/87
1634 + 269	3C342	Q	0.561	16:34:34.22	+26:54:10.0	C, 15 GHz	1.42 x 1.26, −86	1/87
1819 + 228	4C22.47	Q	0.628	18:19:07.81	+22:49:45.7	C, 15 GHz	1.78 x 1.36, 88	1/87
1828 + 487	3C380	Q	0.692	18:28:13.55	+48:42:40.4	C, 15 GHz	2.05 x 1.25, 76	1/87
2005 − 044	3C407	Q	0.589	20:05:46.29	−04:27:17.0	C, 15 GHz	1.36 x 1.35, 44	1/87
2349 + 327	4C32.69	Q	0.659	23:49:48.94	+32:47:18.3	C, 15 GHz	1.37 x 1.36, −46	1/87

Table 2. 8.4 GHz observations (A/B array) – observational parameters

(1)	(2)	(3)	(4)	(5)	(6)	(7)	(8)	(9)
Source	Alt. name	Type	z	RA (h m s)	DEC (° ′ ″)	VLA conf.	Beam (″, °)	Epoch
0128 + 061	3C44	G	0.660	01:28:45.20	06:08:15.0	B, 8.4 GHz	0.84 x 0.78, −57	12/91
0340 + 048	3C93	Q	0.358	03:40:51.50	04:48:21.7	B, 8.4 GHz	0.82 x 0.77, −56	12/91
0528 + 064	3C142.1	G	0.406	05:28:48.10	06:28:14.8	B, 8.4 GHz	0.68 x 0.63, −36	12/91
0610 + 260	3C154	Q	0.580	06:10:43.75	26:05:30.0	B, 8.4 GHz	0.77 x 0.66, −66	12/91
0710 + 118	3C175	Q	0.768	07:10:15.38	11:51:24.0	B, 8.4 GHz	0.78 x 0.71, −61	12/91
0742 + 021	3C187	G	0.350	07:42:27.94	02:07:44.6	B, 8.4 GHz	0.86 x 0.81, −56	12/91
0824 + 294	3C200	G	0.458	08:24:21.43	29:28:42.2	A, 8.4 GHz	0.21 x 0.18, −8	12/92
0838 + 133	3C207	Q	0.684	08:38:01.73	13:23:05.4	B, 8.4 GHz	0.76 x 0.72, −54	12/91
0941 + 100	3C226	G	0.817	09:41:36.20	10:00:05.1	B, 8.4 GHz	0.83 x 0.72, −67	12/91
1508 + 080	3C313	G	0.461	15:08:33.04	08:02:58.5	B, 8.4 GHz	1.16 x 1.05, −52	12/91
1602 + 014	3C327.1	G	0.462	16:02:12.96	01:25:58.7	B, 8.4 GHz	1.14 x 0.91, −60	12/91
2252 + 129	3C455	Q	0.555	22:52:34.53	12:57:33.5	A, 8.4 GHz	0.21 x 0.20, −19	12/92

Table 3. 1.4 GHz observations (A array) – observational parameters

(1)	(2)	(3)	(4)	(5)	(6)	(7)	(8)	(9)
Source	Alt. name	Type	z	RA (h m s)	DEC (° ′ ″)	VLA conf.	Beam (″, °)	Epoch
0035 + 130	3C16	G	0.406	00:35:09.16	13:03:39.6	A, 1.4 GHz	1.19 x 1.15, −31	12/92
0340 + 048	3C93	Q	0.358	03:40:51.50	04:48:21.7	A, 1.4 GHz	1.22 x 1.18, 33	12/92
0528 + 064	3C142.1	G	0.406	05:28:48.10	06:28:14.8	A, 1.4 GHz	1.27 x 1.21, 22	12/92
0610 + 260	3C154	Q	0.580	06:10:43.75	26:05:30.0	A, 1.4 GHz	1.13 x 1.10, 38	12/92
0710 + 118	3C175	Q	0.768	07:10:15.38	11:51:24.0	A, 1.4 GHz	1.21 x 1.18, 30	12/92
0742 + 021	3C187	G	0.350	07:42:27.94	02:07:44.6	A, 1.4 GHz	1.31 x 1.29, 37	12/92
0824 + 294	3C200	G	0.458	08:24:21.43	29:28:42.2	A, 1.4 GHz	1.14 x 1.07, 29	12/92
0838 + 133	3C207	Q	0.684	08:38:01.73	13:23:05.4	A, 1.4 GHz	1.17 x 1.15, −27	12/92
0941 + 100	3C226	G	0.817	09:41:36.20	10:00:05.1	A, 1.4 GHz	1.30 x 1.22, −4	12/92
1508 + 080	3C313	G	0.461	15:08:33.04	08:02:58.5	A, 1.4 GHz	1.40 x 1.35, −28	12/92
1545 + 210	3C323.1	Q	0.264	15:45:31.11	21:01:27.5	A, 1.4 GHz	1.53 x 1.34, −64	12/92
1602 + 014	3C327.1	G	0.462	16:02:12.96	01:25:58.7	A, 1.4 GHz	1.37 x 1.27, −20	12/92

Table 4. 15 GHz observations (C array) – contour levels in units of rms noise

(1)	(2)	(3)	(4)	(5)
Source	Alt. name	Type	rms noise (mJy/beam)	Contour levels
0115 + 027	3C37	Q	0.350	−3,3,6,12,24,48,96,192,330
0155 − 109	PKS	Q	0.350	−3,3,6,12,24,48,96,192,384,465
0159 − 117	3C57	Q	0.350	−3,3,6,12,24,48,96,192,384,768,1248
0222 − 008	4C−00.12	Q	0.200	−3,3,6,12,24,48,96,192,384,574
0349 − 146	3C95	Q	0.200	−3,3,6,12,24,48,96,148
0538 + 498	3C147	Q	1.200	−3,3,6,12,24,48,96,192,384,768,1536
0610 + 260	3C154	Q	0.400	−3,3,6,12,24,48,96,192,384,727
0704 + 384	4C38.20	Q	0.210	−3,3,6,12,24,48,96,192,287
0906 + 430	3C216	Q	0.500	−3,3,6,12,24,48,96,192,384,768,1536
0932 + 022	4C02.27	Q	0.250	−3,3,6,12,24,48,96,192,232
0937 + 391	4C39.27	Q	0.250	−3,3,6,12,24,37
1132 + 303	3C261	Q	0.270	−3,3,6,12,24,48,96,143
1136 − 135	PKS	Q	0.495	−3,3,6,12,24,48,96,192,384,575
1137 + 660	3C263	Q	0.340	−3,3,6,12,24,48,96,192,384,507
1150 + 094	4C09.39	Q	0.340	−3,3,6,12,24,48,96,192,384,650
1156 + 631	4C63.15	Q	0.220	−3,3,6,12,24,48,71
1241 + 166	3C275.1	Q	0.585	−3,3,6,12,24,48,96,192,384,545
1305 + 069	3C281	Q	0.210	−3,3,6,12,24,48,81
1327 − 214	PKS	Q	0.315	−3,3,6,12,24,48,96,192,384,420
1335 − 061	4C−06.35	Q	0.260	−3,3,6,12,24,48,96,192,338
1423 + 242	4C24.31	Q	0.245	−3,3,6,12,24,48,96,192,231
1451 + 097	4C09.52	Q	0.150	−3,3,6,12,24,48,96,192,384,445
1618 + 177	3C334	Q	0.215	−3,3,6,12,24,48,96,192,384,768
1634 + 269	3C342	Q	0.200	−3,3,6,12,24,48,96,192,336
1819 + 228	4C22.47	Q	0.210	−3,3,6,12,24,48,79
1828 + 487	3C380	Q	0.220	−3,3,6,12,24,48,96,192,384,768,914
2005 − 044	3C407	Q	0.360	−3,3,6,12,24,48,96,192,384,483
2349 + 327	4C32.69	Q	0.200	−3,3,6,12,24,48,96,108

Table 5. 8.4 GHz observations (A/B array) – contour levels in units of rms noise

(1)	(2)	(3)	(4)	(5)
Source	Alt. name	Type	rms noise (mJy/beam)	Contour levels
0128 + 061	3C44	G	0.030	−3,3,6,12,24,48,96,192,384,768,1536,1606
0340 + 048	3C93	Q	0.060	−3,3,6,12,24,48,96,192,384,768,833
0528 + 064	3C142.1	G	0.040	−3,3,6,12,24,48,96,192,356
0610 + 260	3C154	Q	0.200	−3,3,6,12,24,48,96,192,384,768,1536,1822
0710 + 118	3C175	Q	0.090	−3,3,6,12,24,48,96,192,384,702
0742 + 021	3C187	G	0.035	−3,3,6,12,24,48,96,113
0824 + 294	3C200	G	0.060	−3,3,6,12,24,48,96,113
0838 + 133	3C207	Q	0.200	−3,3,6,12,24,48,96,192,384,768,1536,3072,3117
0941 + 100	3C226	G	0.050	−3,3,6,12,24,48,96,192,384,768,1500
1508 + 080	3C313	G	0.100	−3,3,6,12,24,48,96,192,384,720
1602 + 014	3C327.1	G	0.060	−3,3,6,12,24,48,96,192,384,768,1146
2252 + 129	3C455	Q	0.090	−3,3,6,12,24,48,96,192,346

Table 6. 1.4 GHz observations (A array) – contour levels in units of rms noise

(1)	(2)	(3)	(4)	(5)
Source	Alt. name	Type	rms noise (mJy/beam)	Contour levels
0035 + 130	3C16	G	0.150	−3,3,6,12,24,48,96,192,315
0340 + 048	3C93	Q	0.120	−3,3,6,12,24,48,96,192,384,768,1536,1923
0528 + 064	3C142.1	G	0.350	−3,3,6,12,24,48,96,192,384,544
0610 + 260	3C154	Q	0.300	−3,3,6,12,24,48,96,192,384,768,1536,2060
0710 + 118	3C175	Q	0.190	−3,3,6,12,24,48,96,192,384,768,1536,2063
0742 + 021	3C187	G	0.350	−3,3,6,12,24,48,50
0824 + 294	3C200	G	0.180	−3,3,6,12,24,48,96,192,384,768,849
0838 + 133	3C207	Q	0.200	−3,3,6,12,24,48,96,192,384,768,1291
0941 + 100	3C226	G	0.300	−3,3,6,12,24,48,96,192,384,768,1536,1991
1508 + 080	3C313	G	0.550	−3,3,6,12,24,48,96,192,384,708
1545 + 210	3C323.1	Q	0.200	−3,3,6,12,24,48,96,192,384,768,1428
1602 + 014	3C327.1	G	0.230	−3,3,6,12,24,48,96,192,384,768,1536,1627

0340+048 *(3C 93, Fig. 7 & Fig. 8)* Data on this object, one of the nearest 3C quasars, can also be found in Price et al. (1993), who present VLA A array maps at 1.4 and 4.8 MHz frequency. Our 1.4 GHz map shows excellent agreement, while in addition our 8.4 GHz map clearly shows the radio core. Note the symmetric structure of this source and the non-detection of a radio jet at the sensitivities achieved here.

0349−146 *(3C 95, Fig. 9)* Radio images of this large quasar (LAS = 117″) are given by Miley & Hartsuijker (1978; 5.0 GHz WSRT map) and by Price et al. (1993; 1.4 and 8.4 GHz VLA A array maps). Especially their 1.4 GHz VLA image shows more low brightness emission around the southern lobe than our 15 GHz image.

0528+064 *(3C 142.1, Fig. 10 & Fig. 11)* This radio galaxy has no published radio maps. The large double structure is asymmetric and a radio core is seen at 8.4 GHz. The northern radio lobe displays a remarkably sharp inner bound.

0538+498 *(3C 147, Fig. 12)* Radio data at sub-arcsecond resolution of this CSS (Compact Steep Spectrum) quasar can be found at many places in the literature, e.g. in van Breugel et al. (1984; 15 GHz VLA map), Pearson et al. (1985; 8.4 GHz VLA A array map), Spencer et al. (1989; VLA maps at 4.8 and 15 GHz), Akujor et al. (1990; MERLIN maps at 151, 408, 1666, and 4995 MHz), and van Breugel et al. (1992; 22.5 GHz VLA map). Our 15 GHz observation does not resolve the source: published higher resolution observations reveal a complex, two-sided structure.

0610+260 *(3C 154, Fig. 13, Fig. 14 & Fig. 15)* Radio images of this quasar are given by Riley & Pooley (1975), at 5.0 GHz, and by Leahy et al. (1989; 151 MHz MERLIN map, 1.6 GHz VLA B array map). The diffuse emission surrounding the eastern lobe as seen in their images is also present in our 1.4 GHz map, and is nearly missing in our 8.4 and 15 GHz maps.

Table 7. 15 GHz observations (C array) – source parameters

(1)	(2)	(3)	(4)	(5)	(6)	(7)	(8)	(9)
Source	Alt. name	Type	z	F_{15} (mJy)	*LAS* (″)	LIN (kpc)	PA (°)	Comments
0115 + 027	3C37	Q	0.672	246	13	68	74	
0155 − 109	PKS	Q	0.616	306	4.3	22	126	
0159 − 117	3C57	Q	0.669	615	14	74	157	
0222 − 008	4C−00.12	Q	0.687	159	14	72	66	
0349 − 146	3C95	Q	0.614	163	117	598	166	
0538 + 498	3C147	Q	0.545	2426	0.2	1		Compact
0610 + 260	3C154	Q	0.580	633	49	253	50	
0704 + 384	4C38.20	Q	0.579	136	22	112	85	
0906 + 430	3C216	Q	0.670	1004	0.5	2.6		Compact
0932 + 022	4C02.27	Q	0.659	109	46	242	49	
0937 + 391	4C39.27	Q	0.618	45	53	271	134	
1132 + 303	3C261	Q	0.614	105	15	76	140	
1136 − 135	PKS	Q	0.554	642	15.5	77	125	
1137 + 660	3C263	Q	0.652	450	44	229	111	
1150 + 094	4C09.39	Q	0.698	240	5	27	174	
1156 + 631	4C63.15	Q	0.594	76	59	298	55	
1241 + 166	3C275.1	Q	0.557	580	15	75	165	
1305 + 069	3C281	Q	0.599	72	46	235	12	
1327 − 214	PKS	Q	0.528	309	31	150	152	
1335 − 061	4C−06.35	Q	0.625	263	11	57	126	
1423 + 242	4C24.31	Q	0.649	184	21	108	21	
1451 + 097	4C09.52	Q	0.627	113	25	128	61	
1618 + 177	3C334	Q	0.555	276	45.5	225	130	
1634 + 269	3C342	Q	0.561	113	40	198	105	
1819 + 228	4C22.47	Q	0.628	61	23	117	9	
1828 + 487	3C380	Q	0.692	2770	0.9	4.8		Compact
2005 − 044	3C407	Q	0.589	347	20	101	35	
2349 + 327	4C32.69	Q	0.659	102	60	315	155	

Table 8. 1.4 GHz (A array) and 8.4 GHz (A/B array) observations – source parameters

(1)	(2)	(3)	(4)	(5)	(6)	(7)	(8)	(9)	(10)
Source	Alt. name	Type	z	$F_{1.4}$ (mJy)	$F_{8.4}$ (mJy)	*LAS* (″)	LIN (kpc)	PA (°)	Comments
0035 + 130	3C16	G	0.406	1500		78	337	30	
0128 + 061	3C44	G	0.660		153	65	340	13	
0340 + 048	3C93	Q	0.358	2720	358	32	130	43	Core detection
0528 + 064	3C142.1	G	0.406	2360	348	49	212	131	Core detection
0610 + 260	3C154	Q	0.580	4480	979	49	253	99	
0710 + 118	3C175	Q	0.768	2310	383	48	261	55	
0742 + 021	3C187	G	0.350	1050	49	127	508	162	Core detection
0824 + 294	3C200	G	0.458	1850	137	17	78	158	
0838 + 133	3C207	Q	0.684	2570	1125	10	53	101	
0941 + 100	3C226	G	0.817	2240	272	31	171	144	Core detection
1508 + 080	3C313	G	0.461	3020	416	130	596	59	Core detection
1545 + 210	3C323.1	Q	0.264	2280		69	234	20	Jet detection
1602 + 014	3C327.1	G	0.462	4020	626	14	64	110	
2252 + 129	3C455	Q	0.555		432	3.2	16	59	Core/jet detection

0704+384 *(4C 38.20, Fig. 16)* Miley & Hartsuijker (1978) show a 5.0 GHz WSRT image of this quasar, in which more diffuse emission is present than in our 15 GHz image. This is also the case for the 1.4 GHz VLA A array image given by Price et al. (1993), who also present a 8.4 GHz VLA A array image.

0710+118 *(3C 175, Fig. 17 & Fig. 18)* Among the published data on this quasar are a 1.4 GHz VLA B configuration map and a MERLIN 151 MHz map (Leahy et al. 1989). The structure is double-lobed with a core. Traces of a jet protruding southwestwards can be seen in the 1.4 GHz map. An unpublished high dynamic range image (Bridle et al., priv. comm.) confirms the presence of this one-sided jet.

0742+021 *(3C 187, Fig. 19 & Fig. 20)* The only image of this radio galaxy available in the literature is an early epoch 1.4 GHz radio map presented by Fomalont (1971). This object is among the largest radio sources in the 3C catalogue (LAS=127″, corresponding to 500 kpc) and as mentioned our high resolution maps suffer from insensitivity to large scale emission. The northern lobe has a peculiar elongated condensation at the inner face of the radio lobe. Note in our 8.4 GHz map the separation between the optical identification and the possible radio core, casting doubt on the correctness of the identification.

0824+294 *(3C200, Fig. 21 & Fig. 22)* The most remarkable feature of this radio galaxy is the pronounced one-sided jet in our 1.4 GHz map (see also e.g. Burns et al. 1984). This in an unusual feature in powerful radiogalaxies. Our 8.4 GHz map lacks sensitivity for the low level extended emission, but displays nicely the knotty structure of the jet.

0838+133 *(3C 207, Fig. 23 & Fig. 24)* Maps of this quasar at 8.4 and 1.4 GHz taken with the VLA (Garrington et al. 1991) show a rather small, almost linear, fairly symmetric triple source. There is some emission from a one-sided jet towards the east. These structures can be seen in our 1.4 GHz map, but the underlying plateau of low surface brightness emission appears more extended than previously measured.

0906+430 *(3C 216, Fig. 25)* Many radio observations at subarcsecond resolution have been made of this CSS quasar. Radio maps can be found in Pearson et al. (1985; 8.4 GHz VLA A array map), Barthel et al. (1988; 1.4 GHz VLA A array map), Fejes et al. (1992; 408 and 1666 MHz MERLIN maps), and in van Breugel et al. (1992; 1.4 and 15 GHz VLA maps). The map published by Barthel et al. (1988) shows a core component and two weaker, resolved components on either side: we see some evidence for one of those components on the south western side of the radio core in our 15 GHz image. The steep spectrum emission north east of the radio core is not detected in our 15 GHz observation. Van Breugel's (1992) 1.4 GHz map shows a similar morphology as observed by us at 15 GHz, while their 15 GHz map resolves the source into two components, separated by 0.7″.

0932+022 *(4C 02.27, Fig. 26)* Radio data on this quasar can be found in Miley & Hartsuijker (1978; 5.0 GHz WSRT image), Hintzen et al. (1983; 1.4 GHz VLA A array image), Swarup et al. (1984; 8.4 GHz VLA A array image), and in Price et al. (1993; 8.4 GHz VLA A array image). Good agreement with our 15 GHz map is found. The map given by Hintzen et al. (1983) displays more fine scale structure in the southwestern lobe than our 15 GHz image.

0937+391 *(4C 39.27, Fig. 27)* The 5.0 GHz WSRT map of this quasar given by Miley & Hartsuijker (1978) displays more low surface brightness emission between the radio core and the lobes than our 15 GHz image. A 1.4 GHz VLA A array image presented by Price et al. (1993) shows the jet running from the radio core in southeastern direction.

0941+100 *(3C 226, Fig. 28 & Fig. 29)* Since the early 5 GHz maps made with the Cambridge 5 km telescope (Jenkins et al. 1977) no radio data have been published on this galaxy. Our 1.4 GHz and 8.4 GHz maps show a 31″ large triple structure.

1132+303 *(3C 261, Fig. 30)* We could not locate any published radio images of this quasar. The source exhibits a triple structure, with a size of 15″. The brightest feature in our 15 GHz map is likely to be the source core. The radio lobes differ in brightness, the northwestern one being much weaker than the southeastern one. No trace of a jet is found.

1136−135 *(PKS, Fig. 31)* Saikia et al. (1989) present an 8.4 GHz VLA A array image of this quasar. This high resolution map displays more fine scale structure than is present in our 15 GHz image.

1137+660 *(3C 263, Fig. 32)* Miley & Hartsuijker (1978) give a 5.0 GHz WSRT map of this quasar, in which the southeastern component is clearly seen to be the dominant feature. The 151 MHz MERLIN map and the 1.4 GHz VLA B array map in Leahy et al. (1989) reveal the presence of substantial diffuse emission between the radio core and the southeastern component. Bridle et al. (priv. comm.) observe a continuous one-sided jet towards the eastern lobe in this quasar.

1150+094 *(4C 09.39, Fig. 33)* No radio maps of this quasar could be found in the literature. The observed radio morphology is similar to that of 0155−109. The two components are separated by 5″: the northern component, of which the peak position nearly coincides with the op-

tical quasar position, is much brighter than the southern one.

1156+631 *(4C 63.15, Fig. 34)* Price et al. (1993) display 4.8 and 1.4 GHz VLA A array maps of this quasar. Their 1.4 GHz image shows a trail of radio emission running from the southwestern lobe in the direction of the radio core.

1241+166 *(3C 275.1, Fig. 35)* Radio maps of this quasar can be found in Stocke et al. (1985; 8.4 GHz VLA A array). Their image clearly shows the jet towards the northwestern lobe.

1305+069 *(3C 281, Fig. 36)* Swarup et al. (1984) present an 8.4 GHz VLA A array image of this quasar. In our 15 GHz map the radio core is more pronounced due to its flat spectrum.

1327−214 *(PKS, Fig. 37)* Our 15 GHz image displays the triple structure of this quasar more clearly than the 5.0 GHz WSRT map published by Miley & Hartsuijker (1978).

1335−061 *(4C−06.35, Fig. 38)* Hintzen et al. (1983) present a 1.4 GHz A array image of this quasar, which does not show the rotation symmetric structure of the source as seen in our 15 GHz map. However, this structure does show up in the 8.4 GHz VLA A array map given by Price et al. (1993).

1423+242 *(4C 24.31, Fig. 39)* A 1.4 GHz VLA A array map of this quasar is presented by Hintzen et al. (1983), which is in excellent agreement with our image, as is the 8.4 GHz VLA A array map in Price et al. (1993).

1451+097 *(4C 09.52, Fig. 40)* Miley and Hartsuijker (1978) present a 5.0 GHz WSRT map of this quasar, in which more diffuse emission is present than in our 15 GHz map.

1508+080 *(3C 313, Fig. 41 & Fig. 42)* This radio galaxy has earlier been mapped at 8.4 GHz with the VLA in B array by Baum et al. (1988). It is a fairly large object (LAS= 130″) with two co-linear hotspots and backbending lobe emission. Good agreement with our 1.4 GHz map is found. The 8.4 GHz map possibly shows the radio core.

1545+210 *(3C 323.1, Fig. 43)* Despite the fact that this is one of the nearest radio-loud quasars, few published high quality radio maps exist. The triple structure of this object has been known since the early 5 GHz map by Pooley & Henbest (1974). A more recent map of this 69″ large source can be found in Swarup et al. (1984) who presented a VLA A array map at 8.4 GHz. Gower & Hutchings (1984) finally present a 1.4 GHz VLA A array image. None of these maps, however, displays the radio jet leading into the southern lobe, as seen in our 1.4 GHz map.

1602+014 *(3C 327.1, Fig. 44 & Fig. 45)* Our map at 8.4 GHz is compatible with earlier data at that frequency taken with the VLA in B array (Baum et al. 1988). Both maps show a luminous radio galaxy with a hotspot in each lobe and a core. There appears to be significant low surface brightness emission.

1618+177 *(3C 334, Fig. 46)* This is a well observed quasar. Maps can be found in Miley & Hartsuijker (1978; 5.0 GHz WSRT map), Hintzen et al. (1983; 1.4 GHz VLA A array map), Swarup et al. (1984; 8.4 GHz VLA A array map), Leahy et al. (1989; 151 MHz MERLIN map, 1.4 GHz VLA B array map), and in Price et al. (1993; 8.4 GHz VLA A array map). The images in Leahy et al. (1989) exhibit substantial low surface brightness emission between the radio core and the lobes. Bridle et al. (priv. comm.) observe a continuous one-sided jet towards the eastern lobe in this quasar.

1634+269 *(3C 342, Fig. 47)* A 5.0 GHz WSRT image of this quasar, which is in good agreement with our 15 GHz map, can be found in Miley and Hartsuijker (1978).

1819+228 *(4C 22.47, Fig. 48)* Hintzen et al. (1983) give a 1.4 GHz VLA A array image of this quasar. This map shows substantial low surface brightness emission between the core and the lobes which is not picked up in our 15 GHz observations.

1828+487 *(3C 380, Fig. 49)* Radio maps at subarcsecond resolution of this complex CSS quasar can be found in Pearson et al. (1985; 8.4 GHz VLA A array map), Akujor et al. (1991; 5 GHz MERLIN map), and in van Breugel et al. (1992; 1.4 GHz VLA map). The image given in Pearson et al. (1985) displays more complex fine scale structure than our 15 GHz image.

2005−044 *(3C 407, Fig. 50)* This triple quasar shows a bright radio core, a fairly bright southwestern lobe, a diffuse northeastern lobe, and a knotty jet pointing towards this latter feature. The 8.4 and 1.4 GHz VLA A array images in Price et al. (1993) are in good agreement with our 15 GHz map.

2252+129 *(3C 455, Fig. 51)* Few high quality radio data of this quasar have been published, except MERLIN maps at 1666 MHz (Spencer et al. 1989) and at 4.8 GHz (Akujor et al. 1991). The largest angular size of only 3.2″ and the steep radio spectrum have led to a qualification as compact steep spectrum source. Our 8.4 GHz map at 0.2″ resolution recalls the double morphology but, due the higher sensitivity of the VLA, a core and a one-sided jet pointing towards the southwest show up.

2349+327 *(4C 32.69, Fig. 52)* The radio image of this quasar given by Potash & Wardle (1980), who used the partially completed VLA at 8.4 GHz, agrees with our

Table 9. Radio core parameters at 8.4 GHz

(1)	(2)	(3)	(4)	(5)	(6)	(7)
Source	Alt. name	Type	z	RA (h m s)	DEC (° ′ ″)	Core flux (mJy)
0340 + 048	3C93	Q	0.358	03:40:51.54	04:48:21.6	3.9
0528 + 064	3C142.1	G	0.406	05:28:48.06	06:28:16.7	2.2
0742 + 021	3C187	G	0.350	07:42:28.55	02:07:27.1	3.6
0941 + 100	3C226	G	0.817	09:41:36.21	10:00:05.0	3.7
1508 + 080	3C313	G	0.461	15:08:33.14	08:03:07.7	0.9
2252 + 129	3C455	Q	0.555	22:52:34.54	12:57:33.4	1.4

15 GHz map: although we loose some of the extended emission, the jet is very well defined and exhibits the same curvature as seen in the Potash & Wardle (1980) image. The jet is even better defined in the 1.4 GHz VLA A array image of Price et al. (1993), who also present a 8.4 GHz VLA A array map.

4. Discussion

The radio sources presented in this paper form two independent samples. These samples span a range of properties and were imaged with different purposes. Full discussions of the samples will therefore be given elsewhere. We have here presented total intensity maps and listed the basic source parameters of 41 radio galaxies and quasars. The main new results can be summarized as follows: new, first time (to our knowledge) radio maps were produced of 3C 44, 3C 142.1, 3C 261, 4C 09.39 and PKS 0155−109. Our images furthermore reveal the existence of jets in 3C 323.1 and 3C 455. New radio cores were detected in 3C 93, 3C 142.1, 3C 187, 3C 226, 3C 313 and 3C 455. Parameters for these cores, obtained from gaussian model fitting to the 8.4 GHz images, are listed in Table 9. Good agreement is found with published optical identifications, except for 3C 187, where our high resolution image casts doubt on the published position.

Finally we note that the cores detected in 3C 93 and 3C 455 are remarkably weak for quasars. Using the fluxes at 1.4 GHz and 4.85 GHz listed in White & Becker (1992) and Becker et al. (1991) we estimate spectral index values for the extended emission in these sources: α=0.91 for 3C 93 and α=0.85 for 3C 455. Adopting a flat core spectrum (α=0), we find core fraction values, defined as the core flux divided by the flux of the extended emission at 4.85 GHz emitted frequency, of log R=−2.4 and log R=−2.8 for 3C 93 and 3C 455 respectively. The distribution of this parameter in Kapahi (1990) shows that these values are among the lowest found for quasars. There is, however, some controversy on the classification of these two quasars. Véron-Cetty & Veron (1991) classify 3C 93 as a Seyfert 1 galaxy due to its absolute magnitude M_V=−22.6, below the quasar break at M_V=−23. This magnitude is calculated from the apparent magnitude m_V=19.17 estimated in Lynds & Wills (1978). We have compared this value with the measurements of the long-term monitoring campaign of Pica et al. (1988). During the period 1971-1986 the source varied within the range $17.27 < m_V < 18.25$, indicating that the Lynds & Wills (1978) measurement was either erroneous or taken during an unusually low state. The average magnitude m_V=17.73 from Pica et al. (1988) translates with our adopted cosmology to M_V=−23.12, which brings this object above the quasar break. The pointlike appearance and broad-lined optical spectrum (Smith & Spinrad 1980) provide further arguments for classifying this object as a quasar. Concerning 3C 455, we note that Spencer et al. (1989) classified this object as a galaxy. The apparent magnitude m_V=19.5 (Arp et al. 1972) corresponds to M_V=−22.3, which would argue for this classification. The object appears rather pointlike in the optical however; spectroscopy is needed to determine its nature. Both 3C 93 and 3C 455 admittedly belong to the fringe of the quasar population.

Acknowledgements. We thank D. Wunker and P. Perley for excellent support in scheduling and calibrating the observations. The assistance of A. Szomoru in streamlining the usage of AIPS is gratefully acknowledged. We thank A. Bridle and C.J. Lonsdale for showing us data prior to publication. PDB acknowledges support from the Royal Netherlands Academy of Arts and Sciences. G.K. Miley was involved in the early stages of this project. This research has made use of the NASA/IPAC extragalactic database (NED) which is operated by the Jet Propulsion Laboratory, Caltech, under contract with the National Aeronautics and Space Administration.

References

Akujor C.E., Spencer R.E., Wilkinson P.N. 1990, MNRAS 244, 362
Akujor C.E., Spencer R.E., Zhang F.J., Davis R.J., Browne I.W.A., Fanti C. 1991, MNRAS 250, 215
Antonucci R.A. 1993, ARA&A 31, 473
Arp H., Burbidge E., Mackay C., Strittmatter P. 1972, ApJ 171, L41
Barthel P.D., Miley G.K. 1988, Nature 333, 319

Barthel P.D., Pearson T.J., Readhead A.C.S. 1988, ApJ 329, L51
Barthel P.D. 1989, ApJ 336, 606
Baum S.A., Heckman T., Bridle A., van Breugel W., Miley G. 1988, ApJS 68, 643
Becker R.H., White R.L., Edwards A.L. 1991, ApJS 75, 1
Bogers W.J., Barthel P.D., Lonsdale C.J., Miley G.K. 1994, in preparation
Burns J.O, Basart J.P., De Young D.S., Ghiglia D.C. 1984, ApJ 283, 515
Downes A.J.B., Peacock J.A., Savage A., Carrie D.R. 1986, MNRAS 218, 31
Fejes I., Porcas R.W., Akujor C.E. 1992, A&A 257, 459
Fomalont E.B. 1971, AJ 76, 513
Garrington S.T., Conway R.G., Leahy J.P. 1991, MNRAS 250, 171
Gower A.C., Hutchings J.B. 1984, AJ 89, 1658
Hes R., Barthel P.D., Fosbury R.A.E. 1993, Nature 362, 326
Hewitt A., Burbidge G. 1987, ApJS 63, 1
Hintzen P., Ulvestad J., Owen F. 1983, AJ 88, 709
Kapahi, V.K. 1990, in: Parsec-scale radio jets, eds. J.A. Zensus and T.J. Pearson, (CUP, Cambridge) p. 304
Leahy J.P., Muxlow T.W.B., Stephens P.W. 1989, MNRAS 239, 401
Leahy J.P., Perley R.A. 1991, AJ 102, 537
Lonsdale C.J., Barthel P.D., Miley G.K. 1993, ApJS 87, 63
Jenkins C.J., Pooley G.G., Riley J.M. 1977, Mem. R. astr. Soc. 84, 61
Miley G.K., Hartsuijker A.P. 1978, A&AS 34, 129
Pearson T.J., Perley R.A., Readhead A.C.S. 1985, AJ 90, 738
Pica A.J., Smith A.G., Webb J.R., Leacock R.J., Clements S., Gombola P.P. 1988, ApJ 96, 1215
Pooley G.G., Henbest S.N. 1974, MNRAS 169, 477
Potash R.I., Wardle J.F.C. 1980, ApJ 239, 42
Price R., Gower A.C., Hutchings J.B., Talon S., Duncan D., Ross G. 1993, ApJS 86, 365
Riley J.M., Pooley G.G. 1975, Mem. R. astr. Soc. 80, 105
Saikia D.J., Cornwell T.J., Muxlow T.W.B. 1989, JA&A 10, 203
Smith, H.E., Spinrad, H. 1980, ApJ 236, 419
Spencer R.E., McDowell J.C., Charlesworth M., Fanti C., Parma P., Peacock J.A. 1989, MNRAS 240, 657
Spinrad H., Djorgovski S., Marr J., Aguilar L. 1985, PASP 97, 932
Stocke J.T., Burns J.O., Christiansen W.A. 1985, ApJ 299, 799
Strom R.G., Conway R.G. 1985, A&AS 61, 547
Swarup G., Sinha R.P., Hilldrup K. 1984, MNRAS 208, 813
Van Breugel W., Miley G., Heckman T. 1984, AJ 89, 5
Van Breugel W.J.M., Fanti, C., Fanti, R., Stanghellini, C., Schilizzi, R.T., Spencer, R.E., 1992, A&A 256, 56
Véron-Cetty, M. P., Véron, P. 1991, A Catalogue of Quasars and Active nuclei (5^{th} Edition), ESO Scientific Report No. 10
White R.L., Becker R.H. 1992, ApJS 79, 331
Wilkinson P.N., Akujor, C.E., Cornwell, T.J., Saikia, D.J. 1991, MNRAS 248, 86

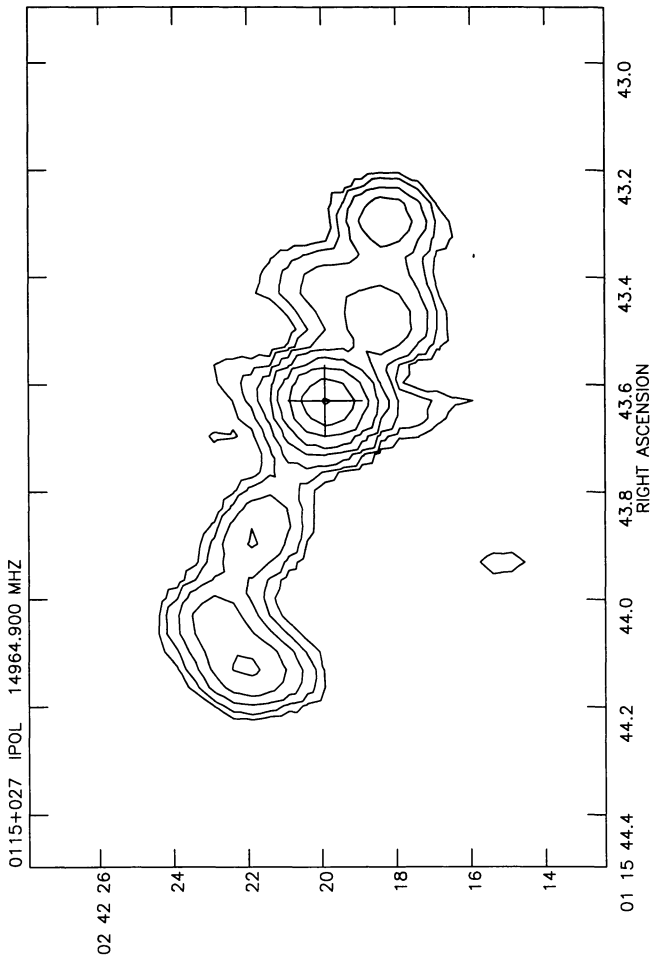

Fig. 2.

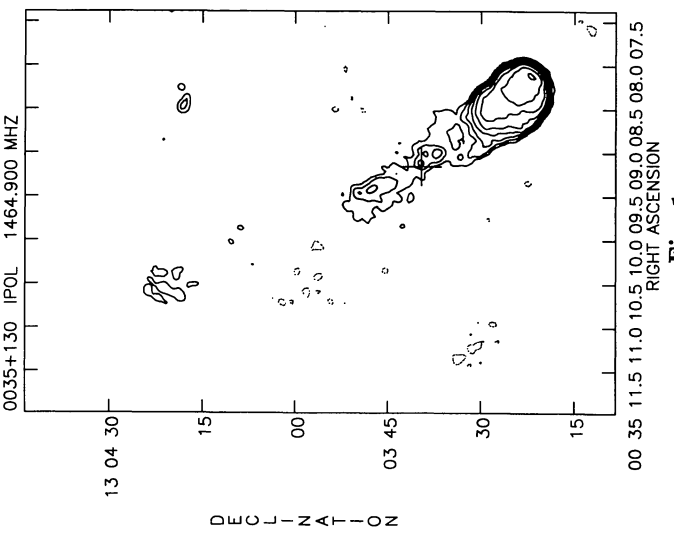

Fig. 1.

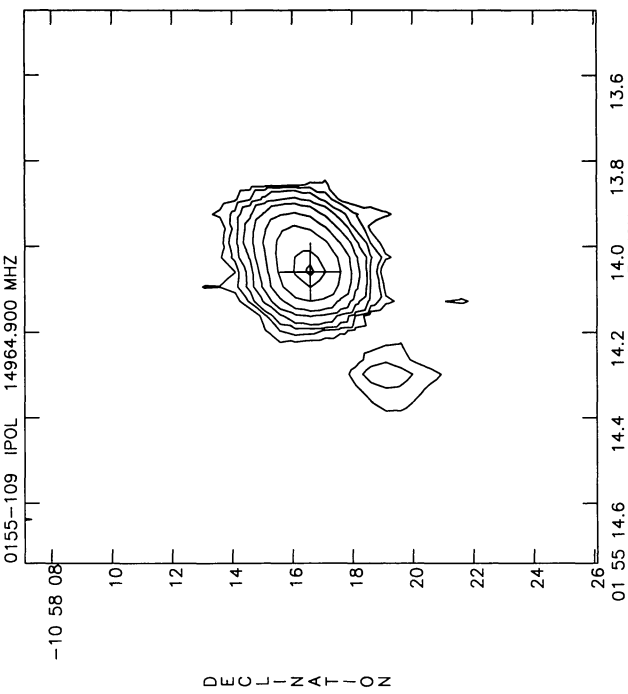

Fig. 4.

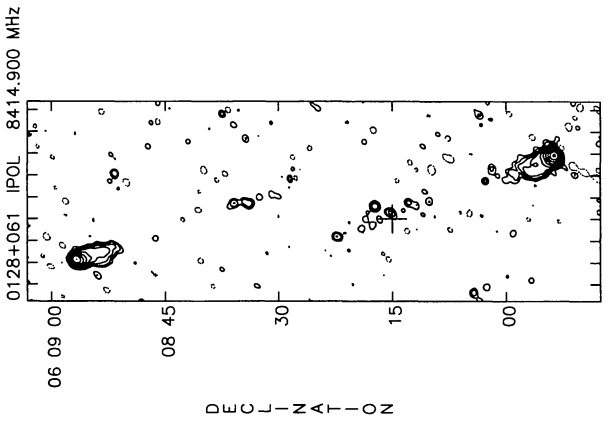

Fig. 3.

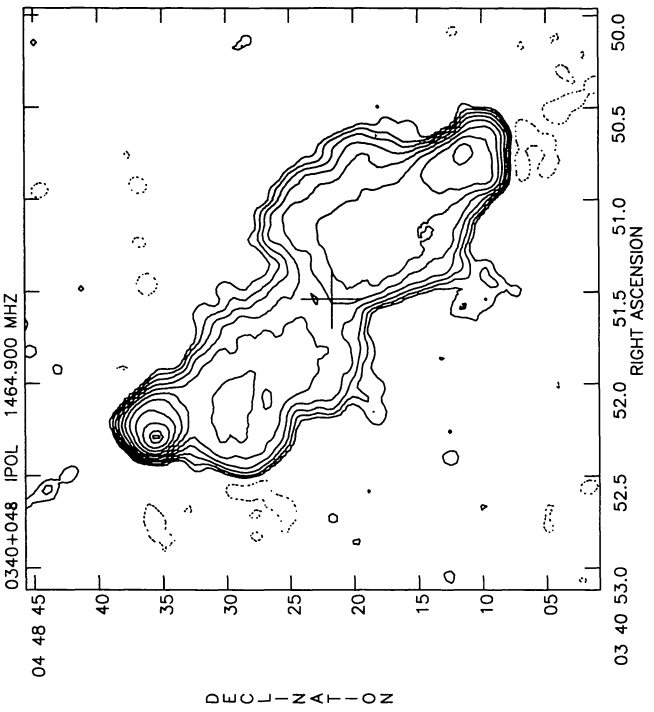

Fig. 7.

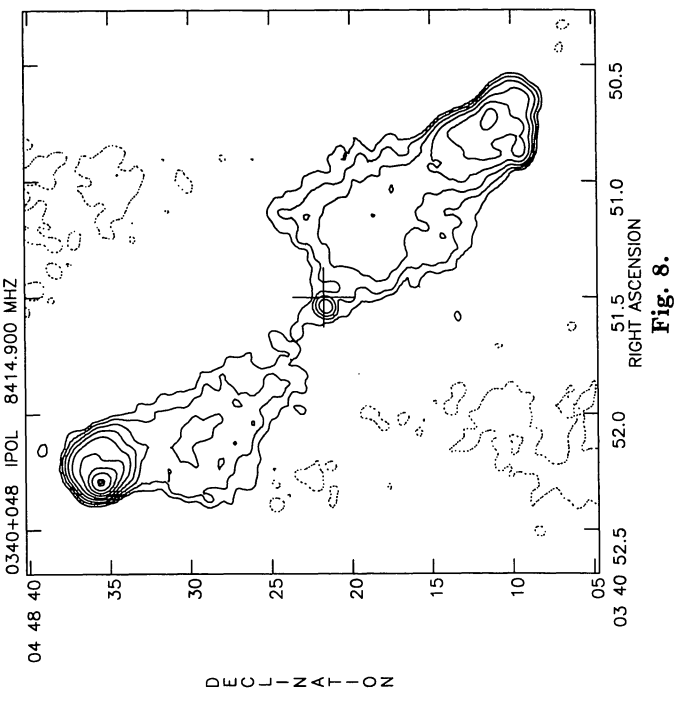

Fig. 8.

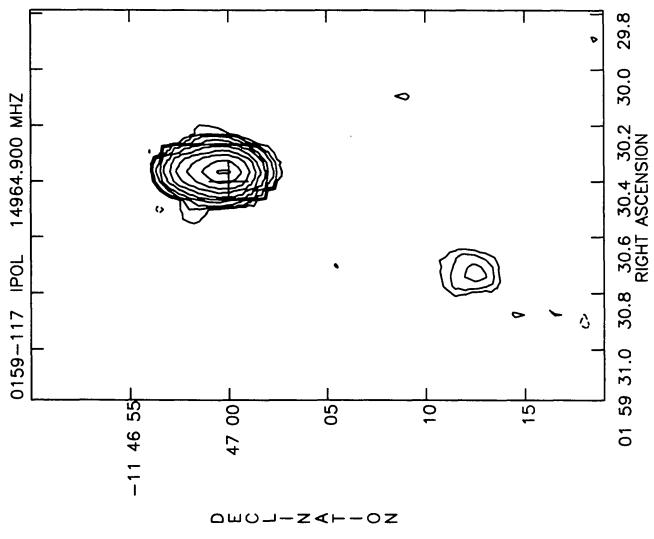

Fig. 5.

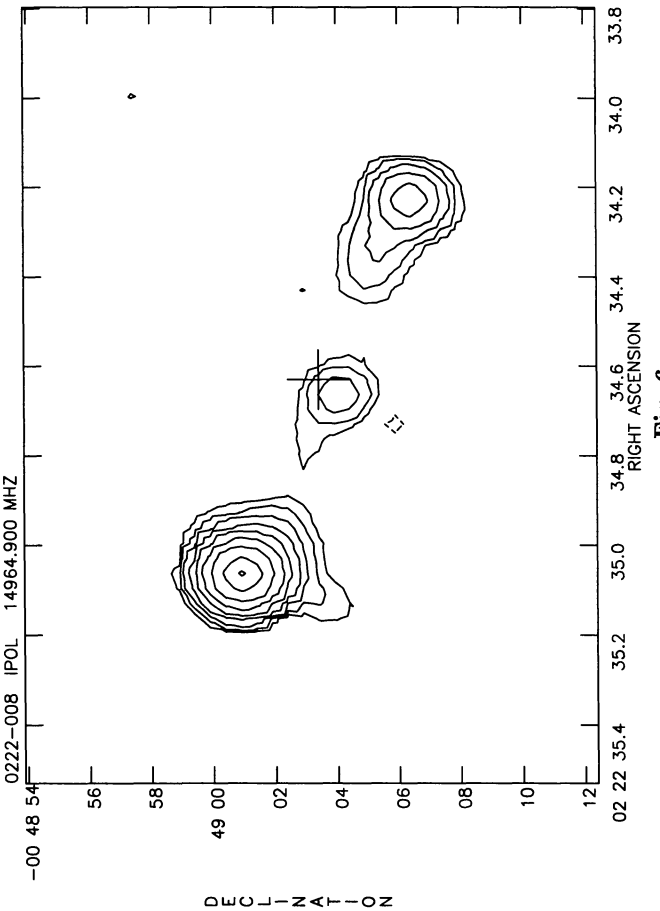

Fig. 6.

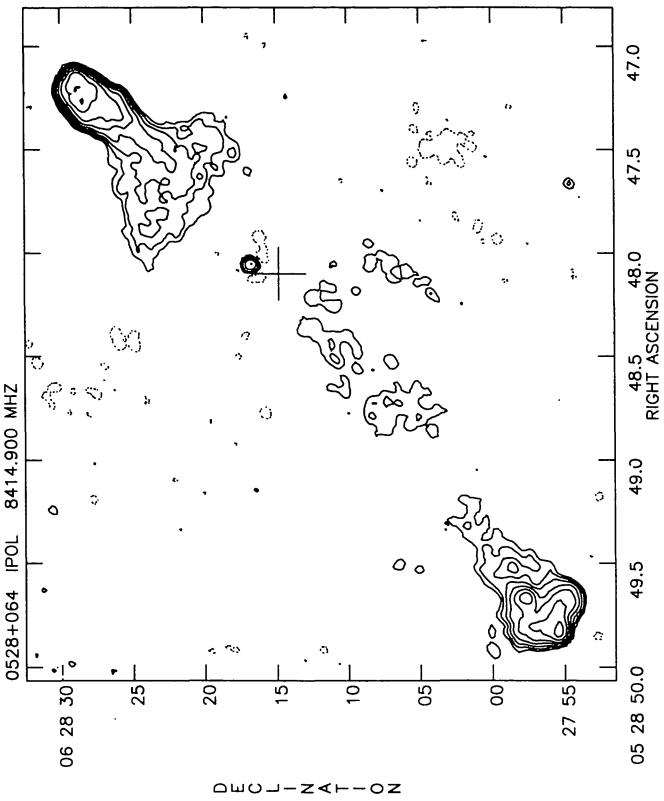

Fig. 11.

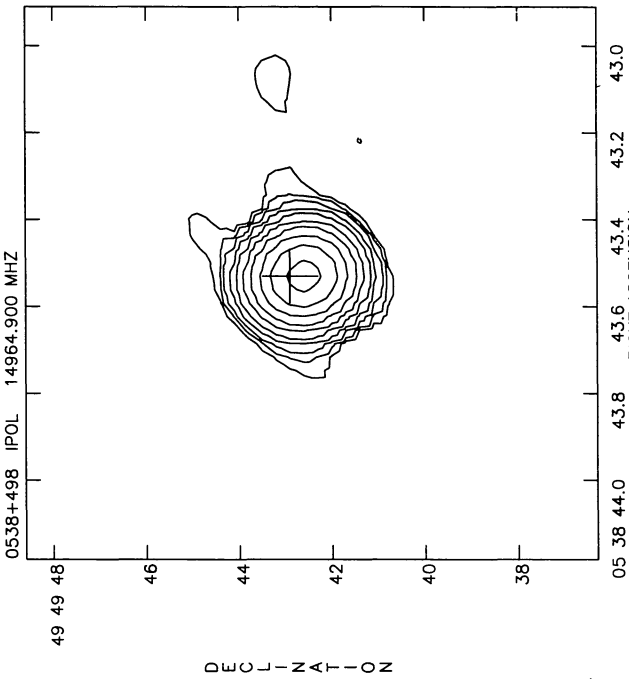

Fig. 12.

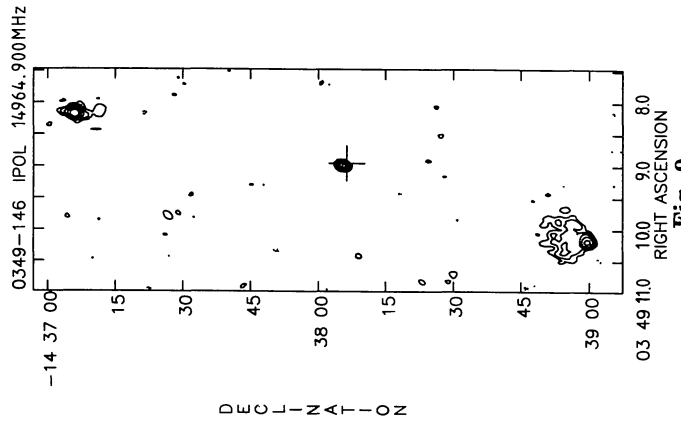

Fig. 9.

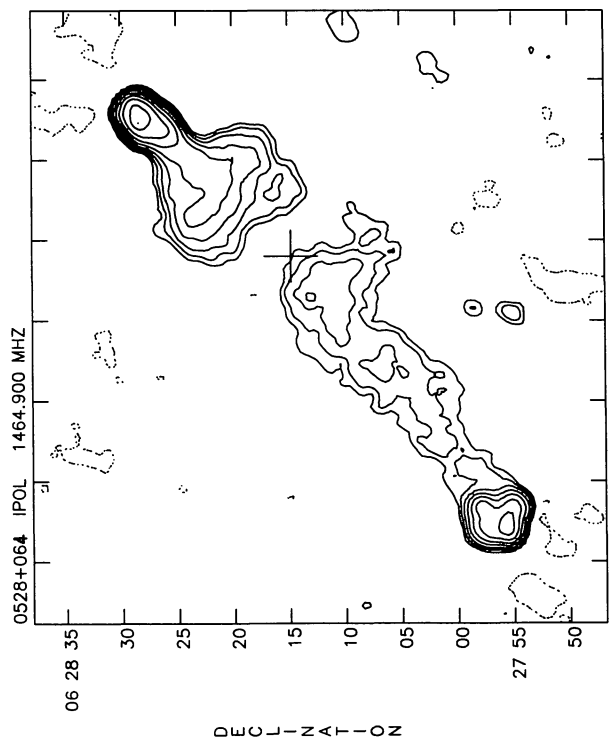

Fig. 10.

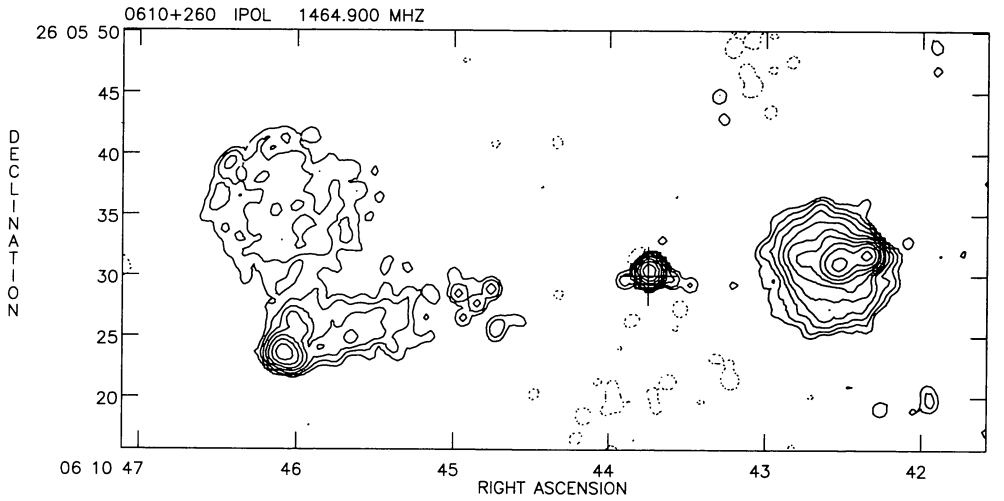

Fig. 13.

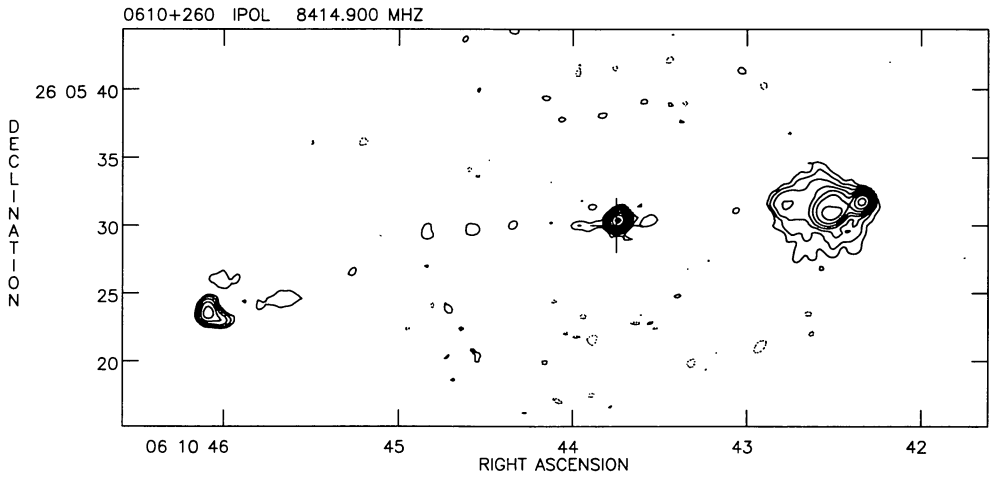

Fig. 14.

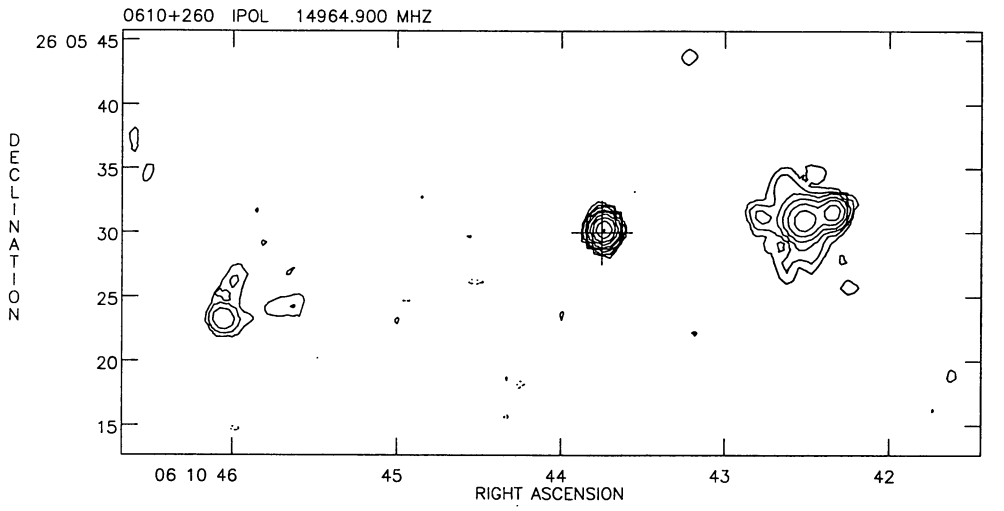

Fig. 15.

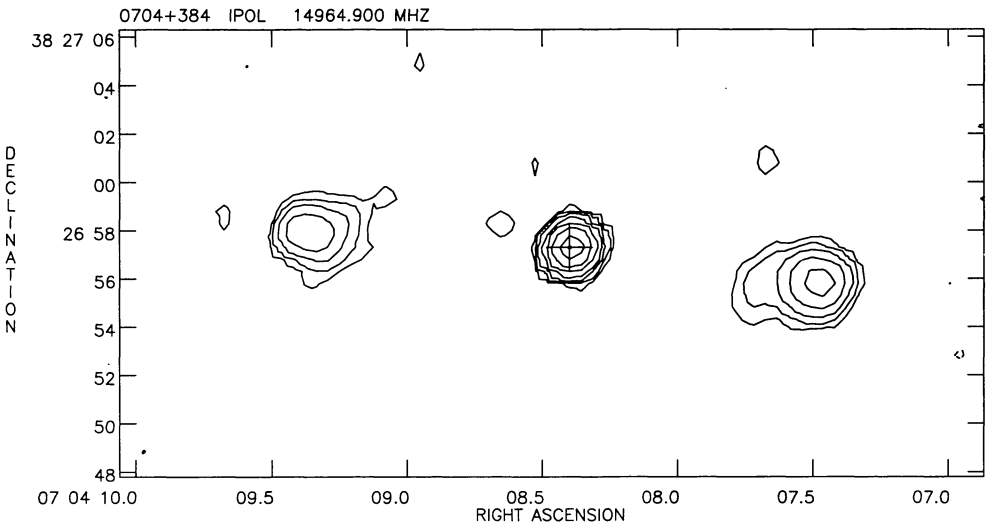

Fig. 16.

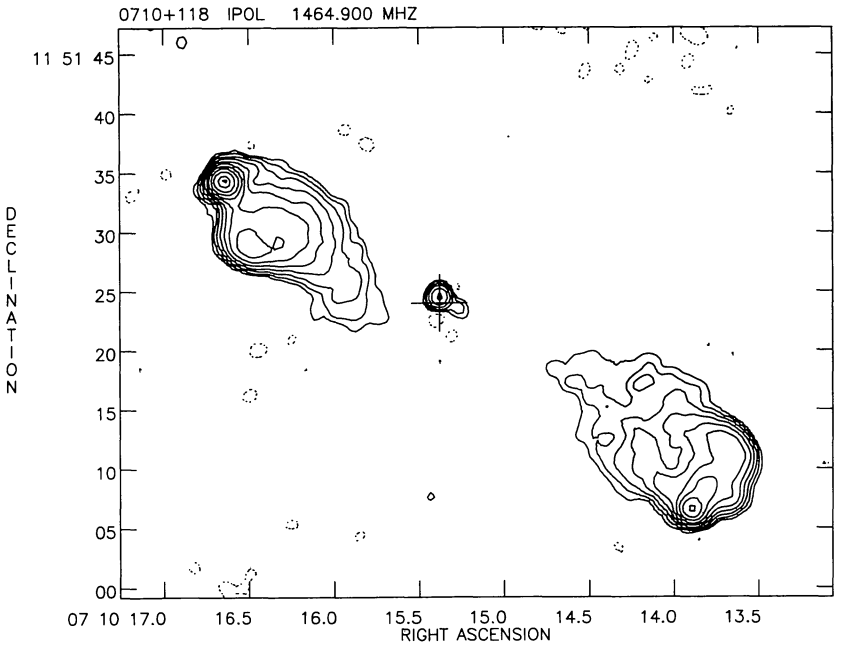

Fig. 17.

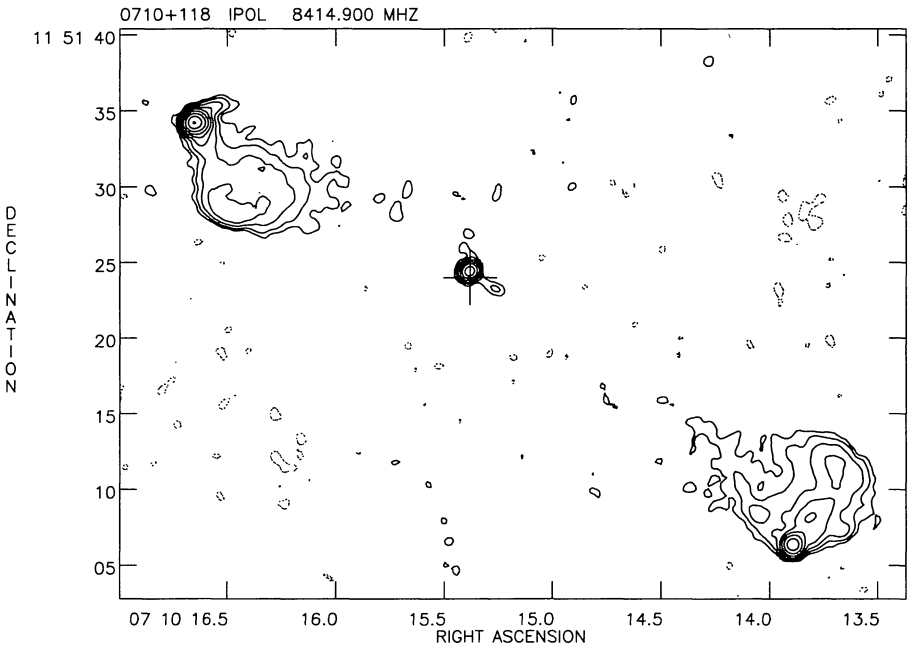

Fig. 18.

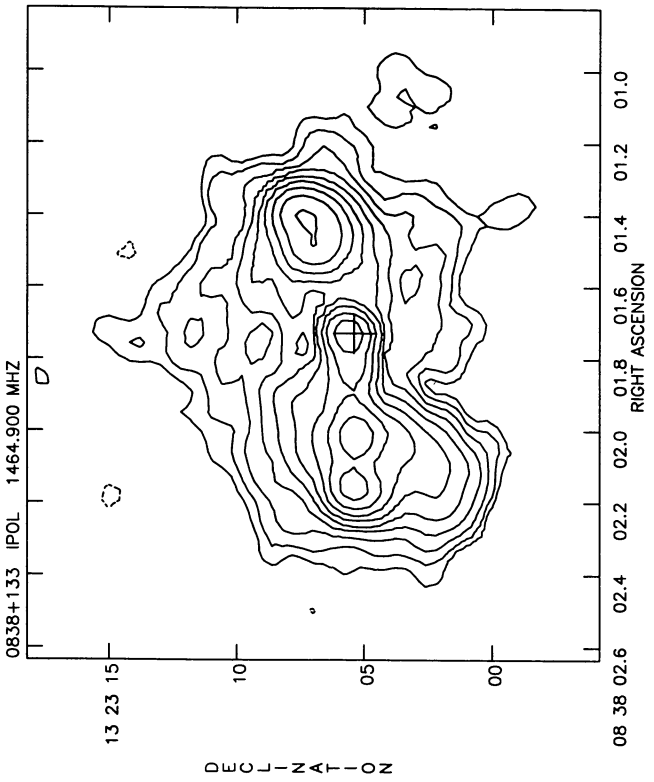

Fig. 23.

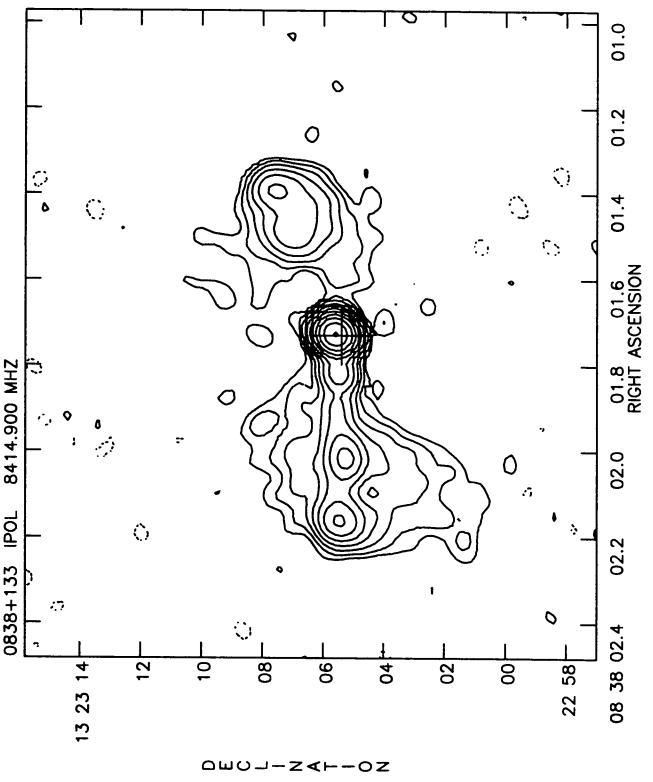

Fig. 24.

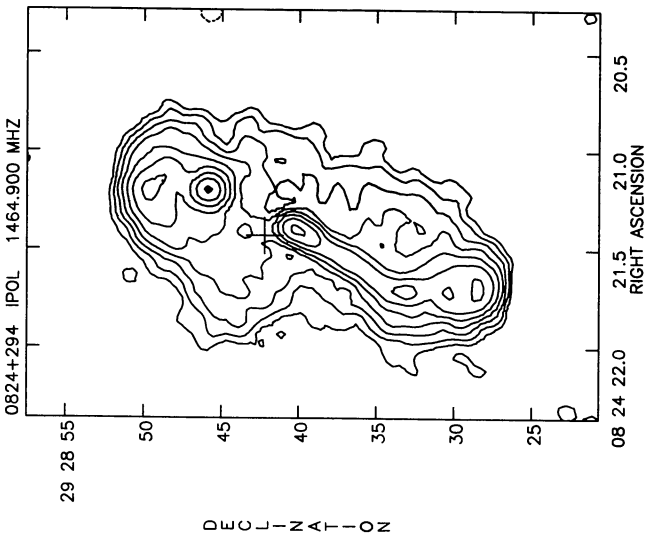

Fig. 21.

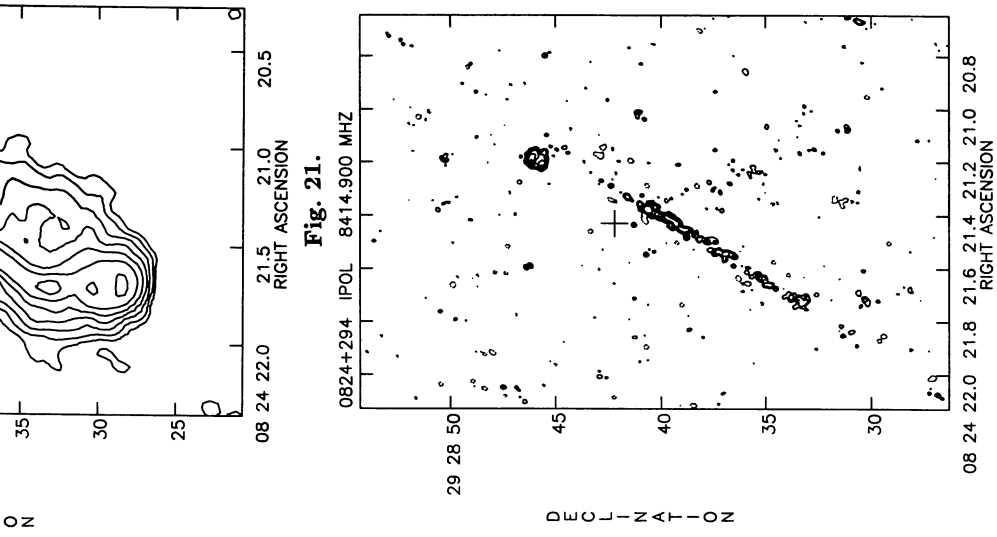

Fig. 22.

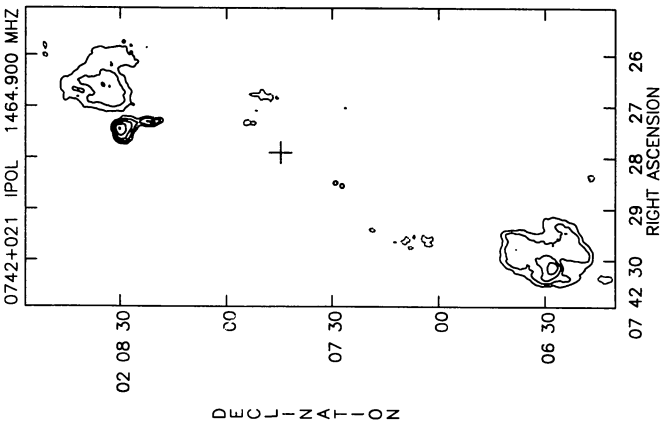

Fig. 19.

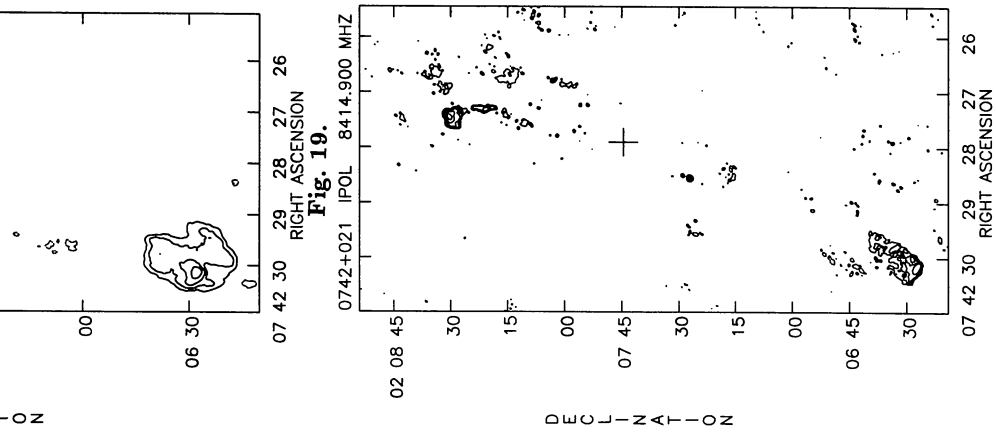

Fig. 20.

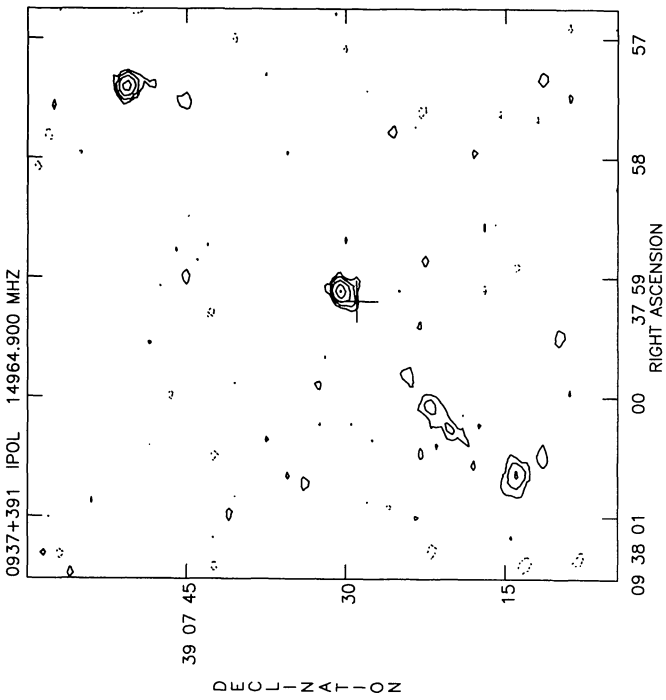

Fig. 27.

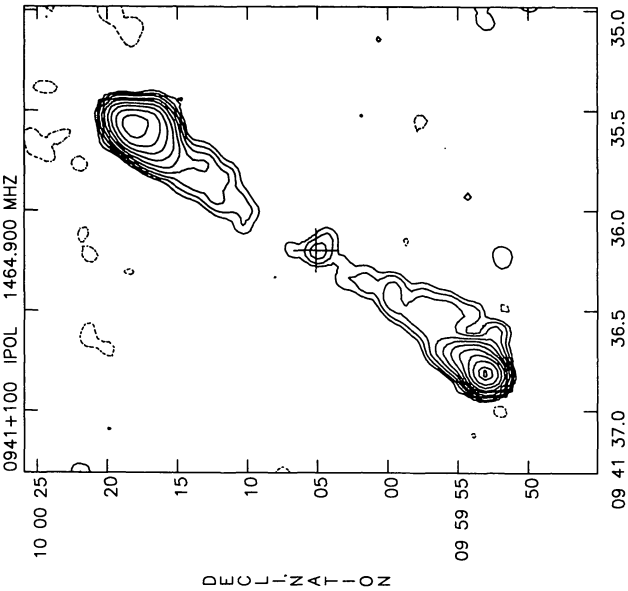

Fig. 28.

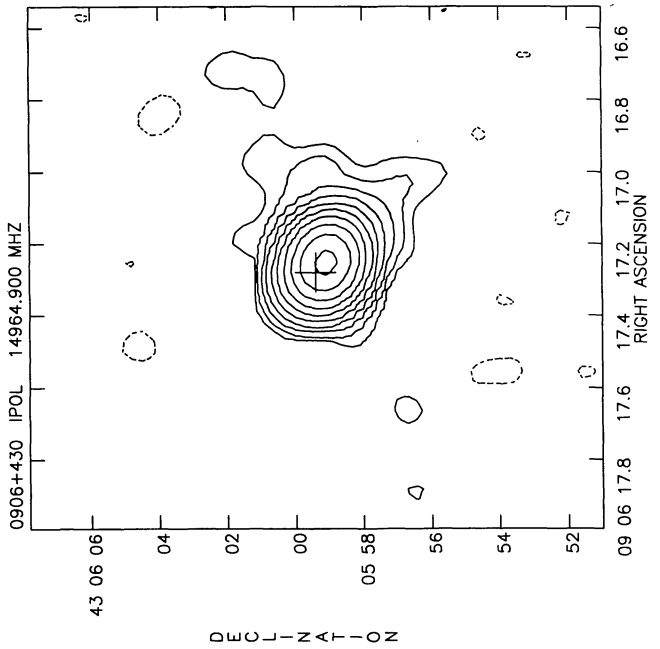

Fig. 25.

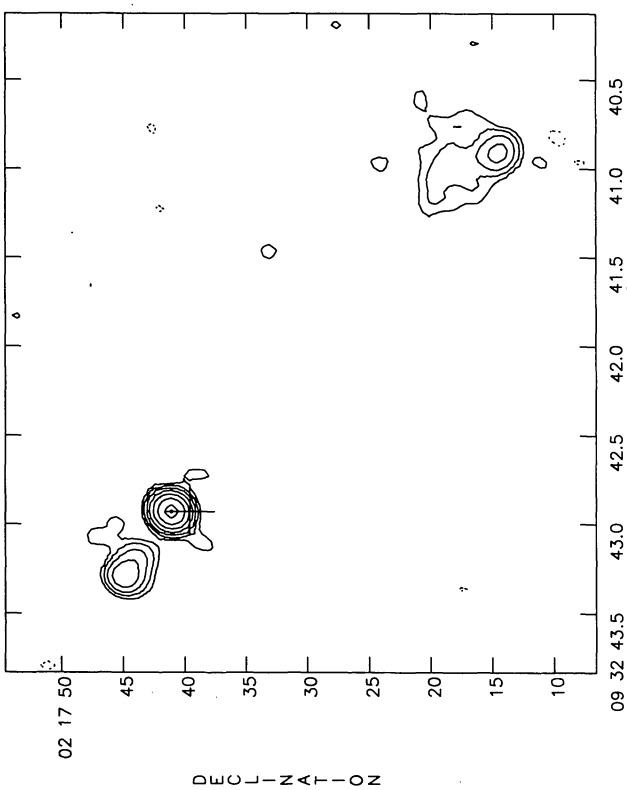

Fig. 26.

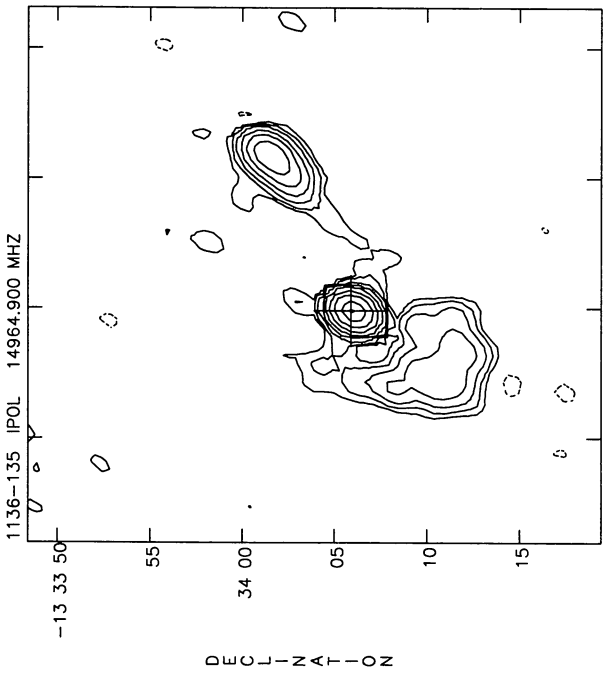

Fig. 31.

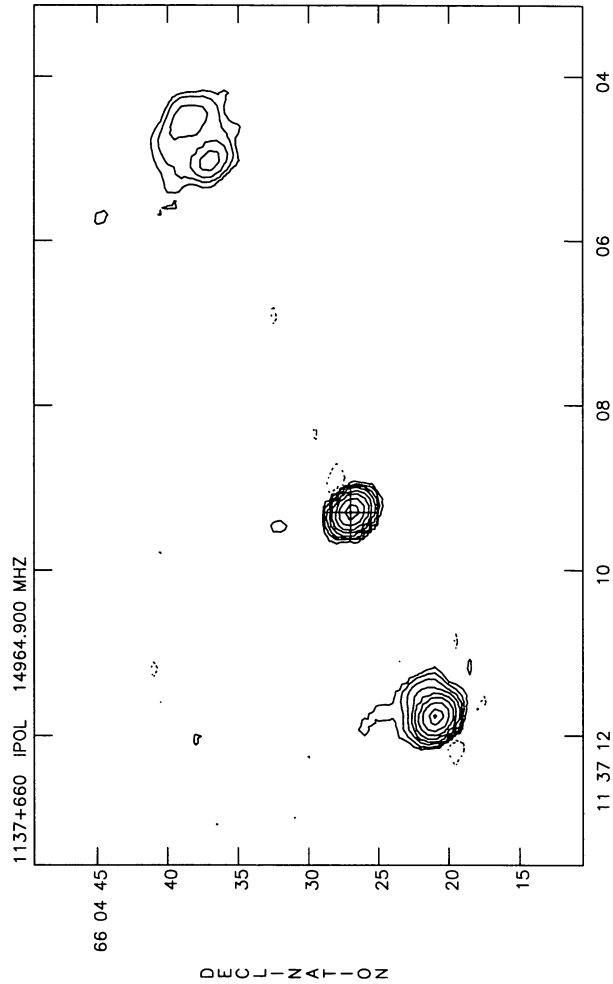

Fig. 32.

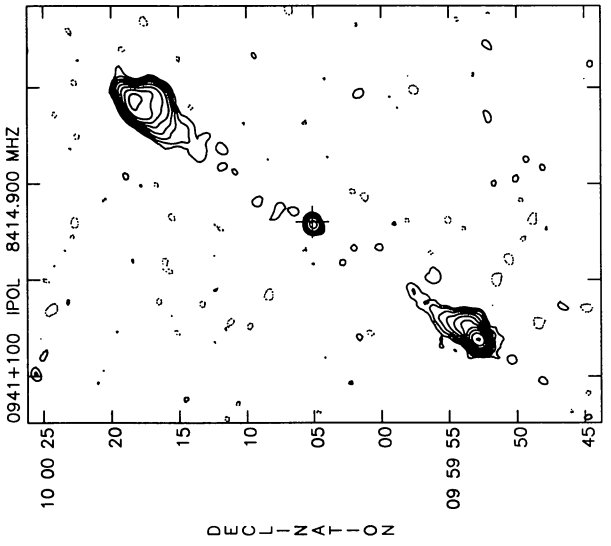

Fig. 29.

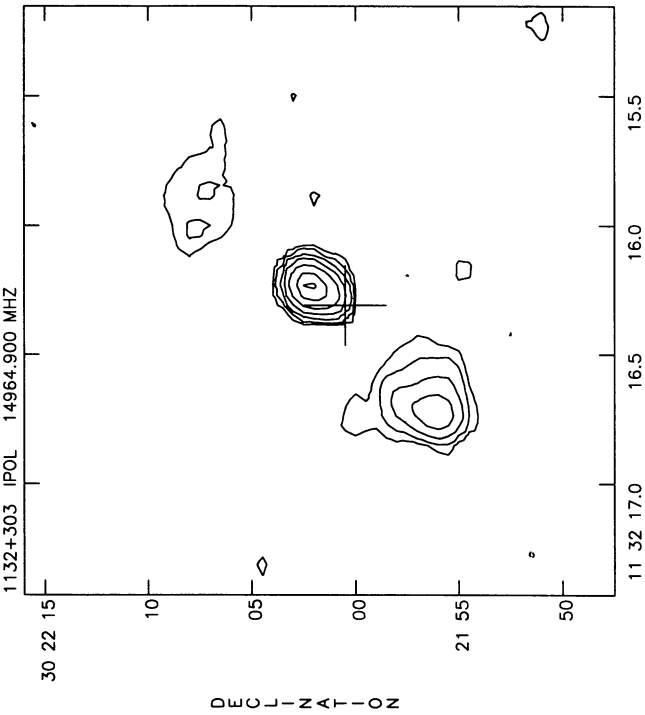

Fig. 30.

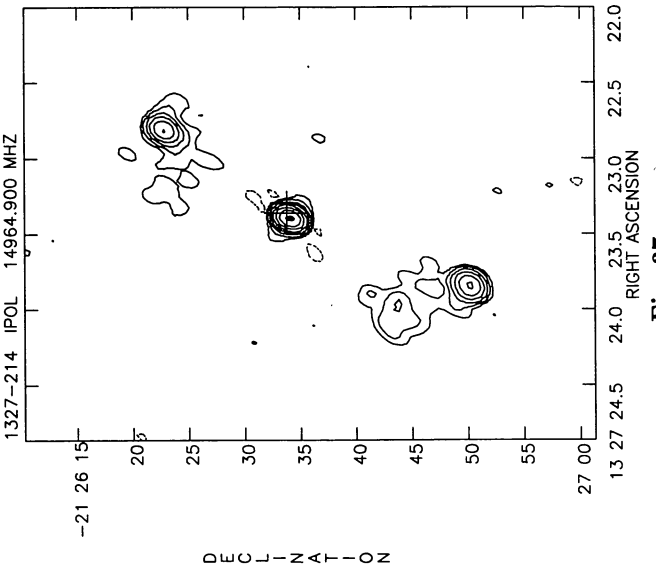

Fig. 37.

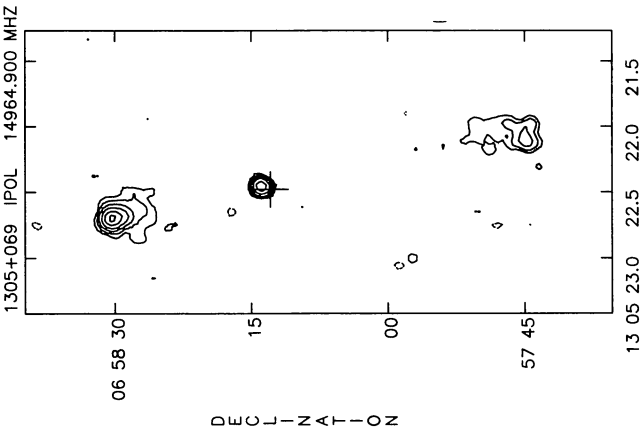

Fig. 36.

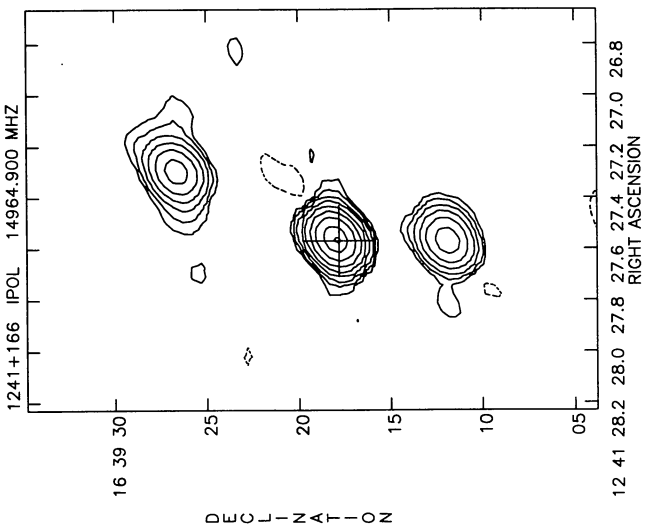

Fig. 35.

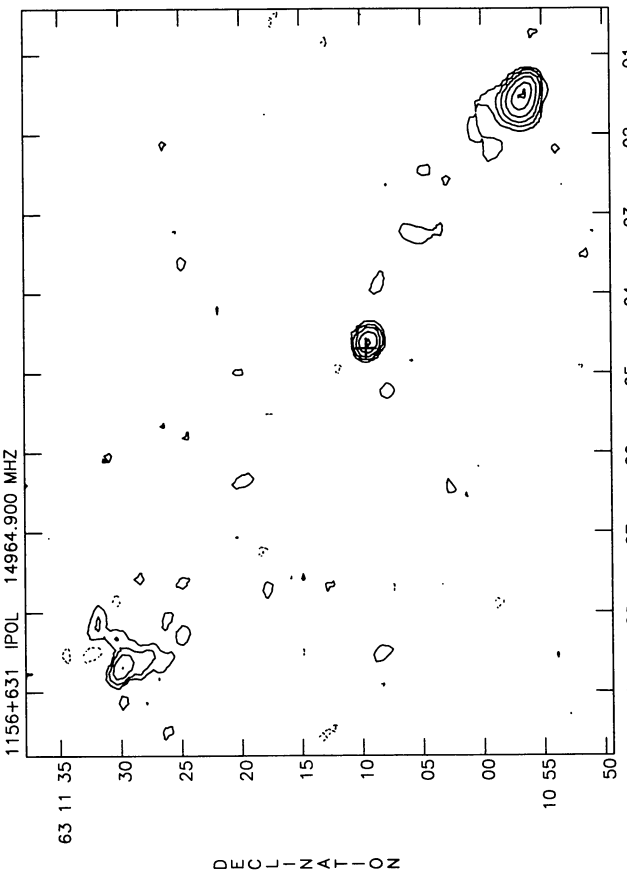

Fig. 34.

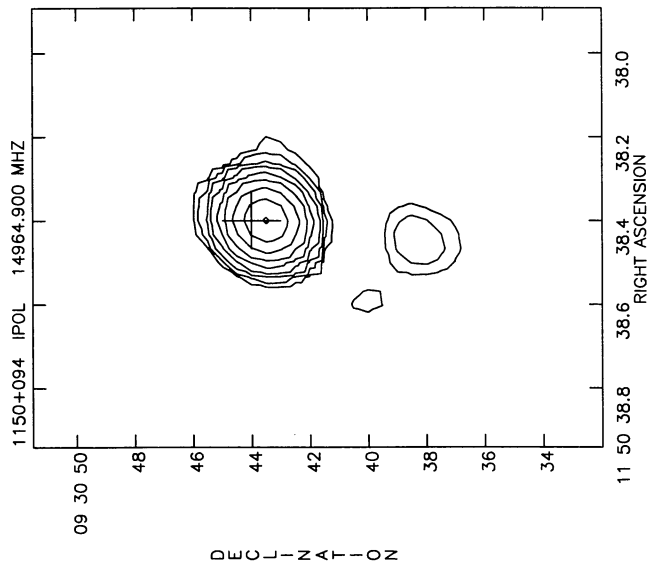

Fig. 33.

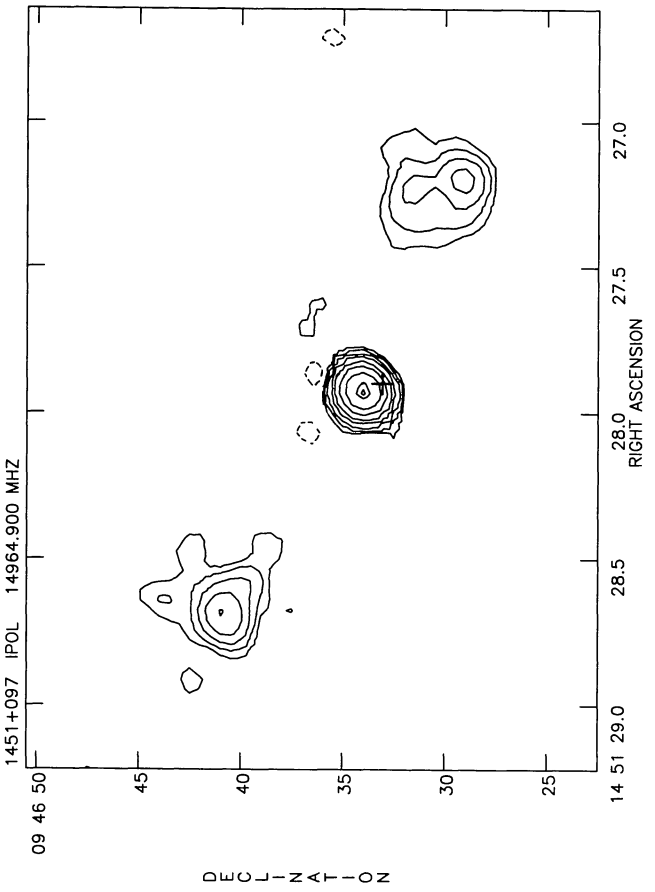

Fig. 40.

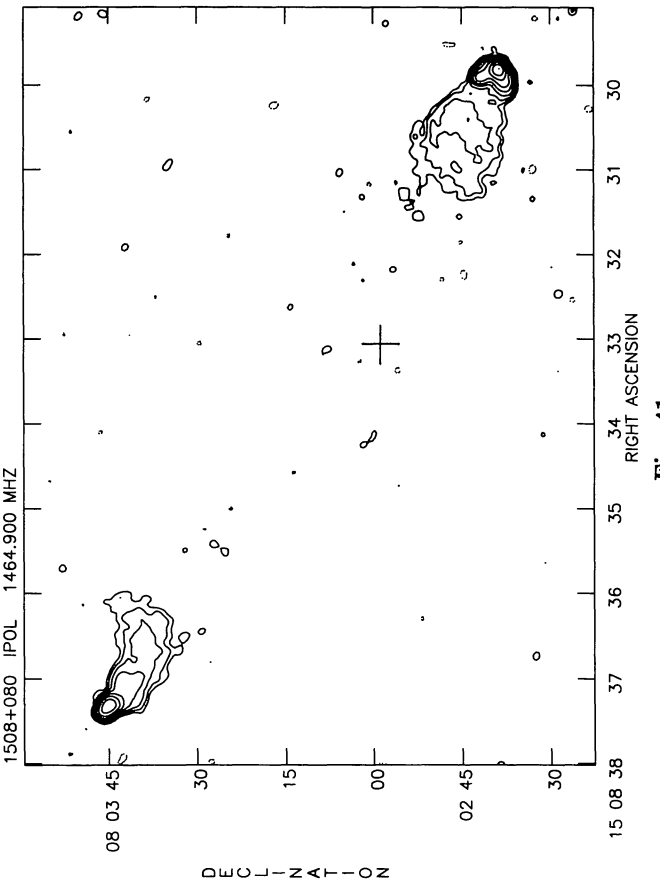

Fig. 41.

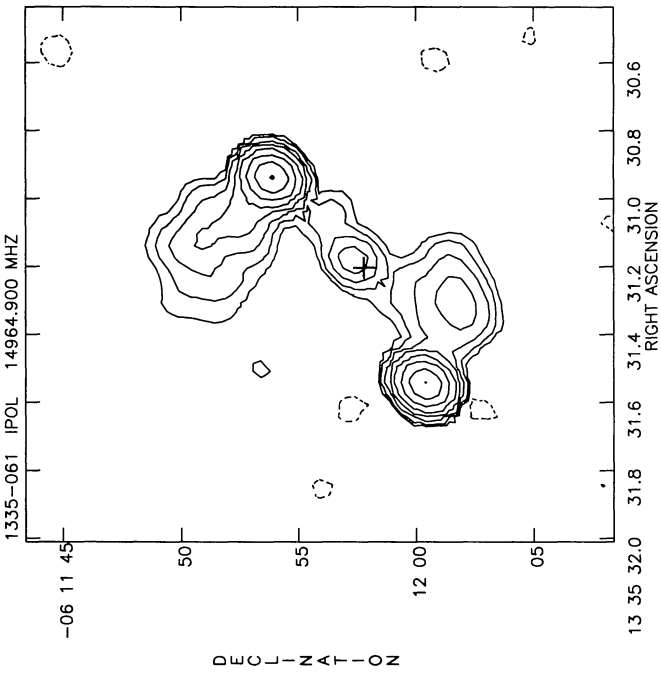

Fig. 38.

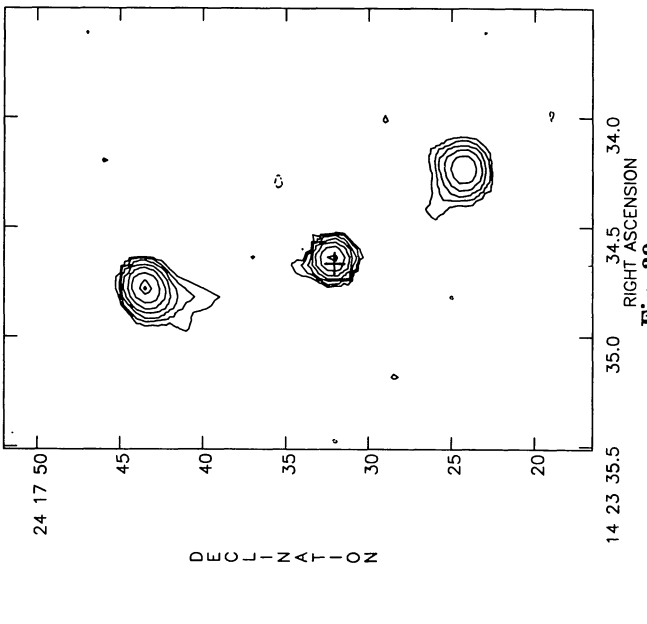

Fig. 39.

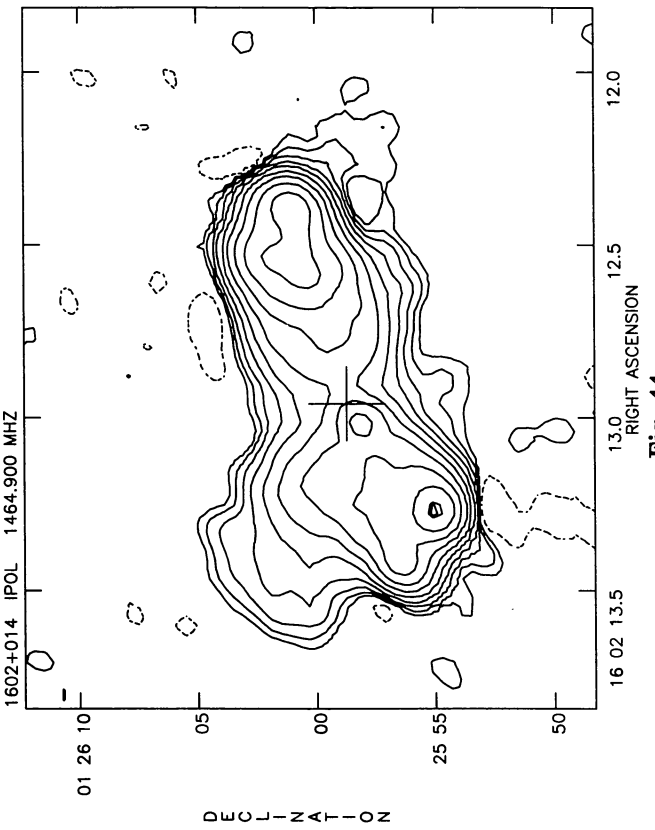

Fig. 44.

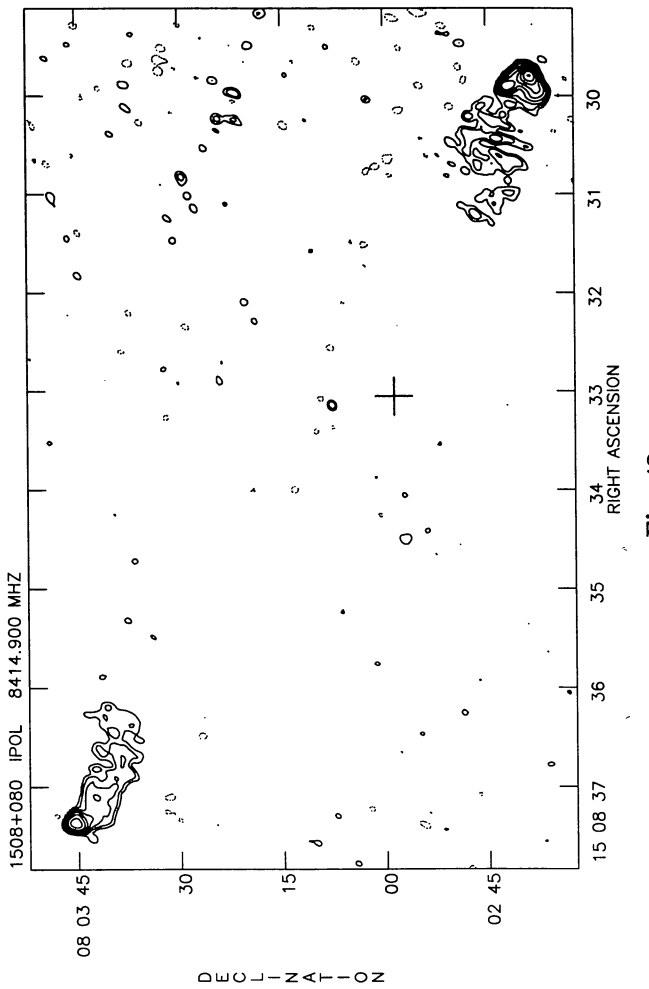

Fig. 42.

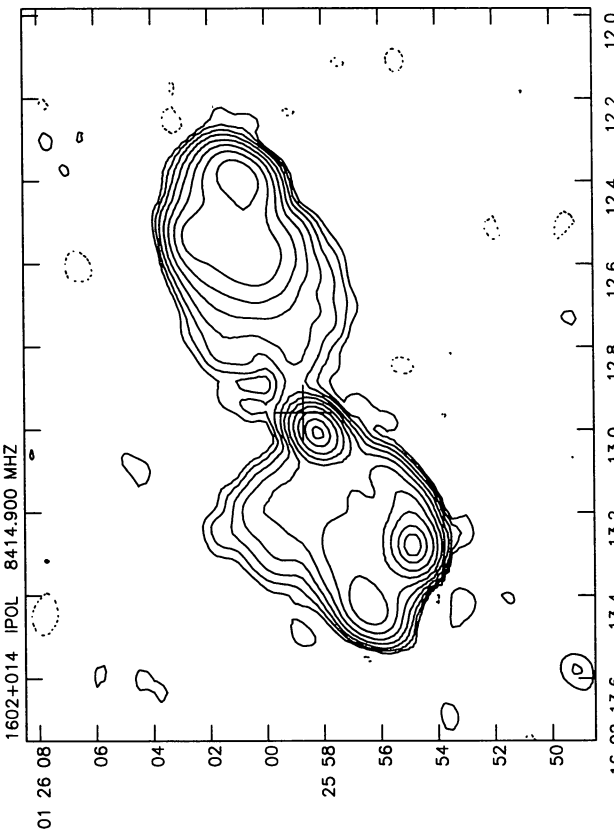

Fig. 45.

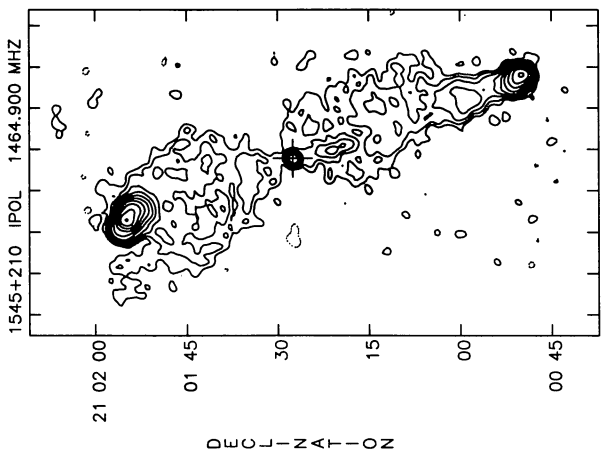

Fig. 43.

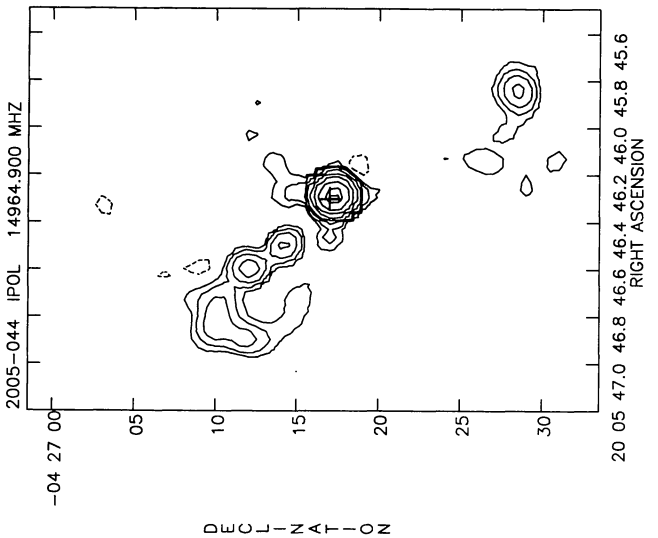

Fig. 50.

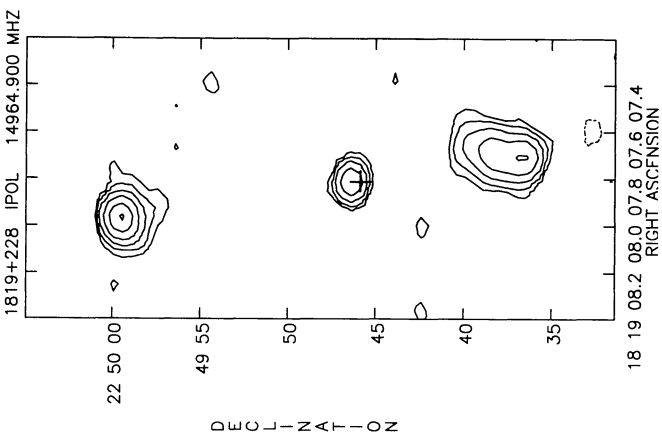

Fig. 48.

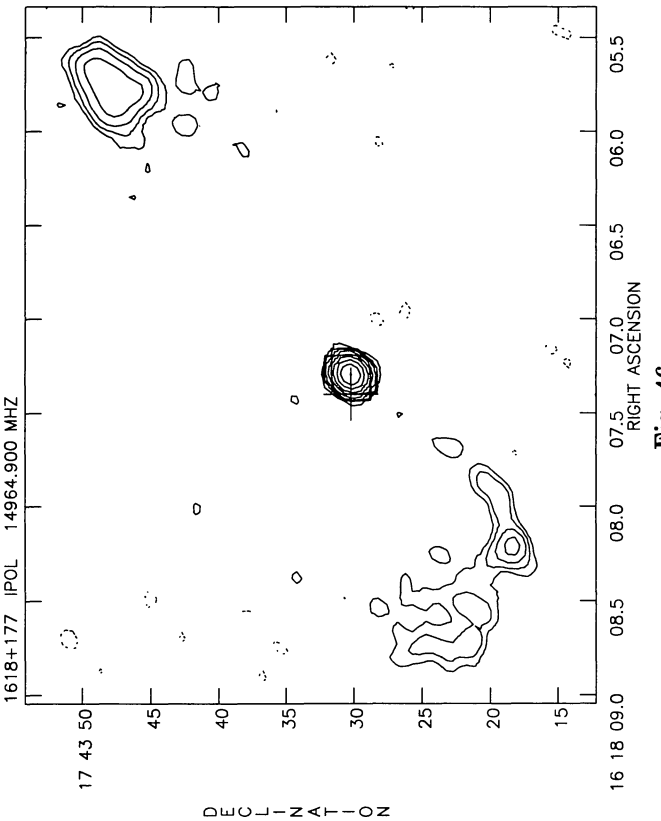

Fig. 46.

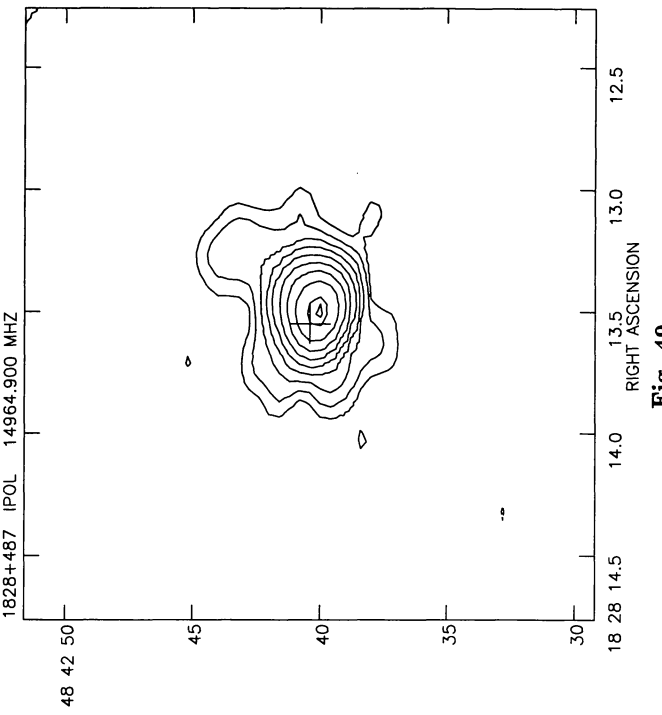

Fig. 49.

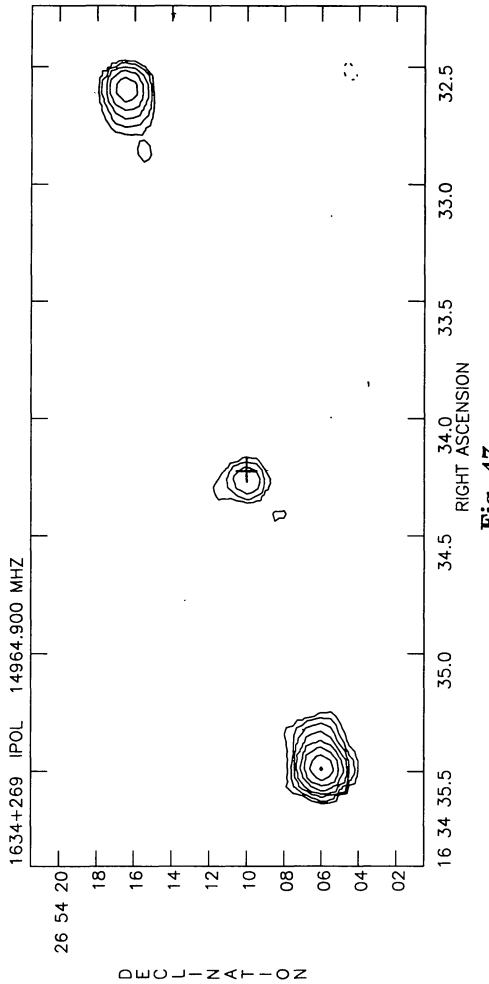

Fig. 47.

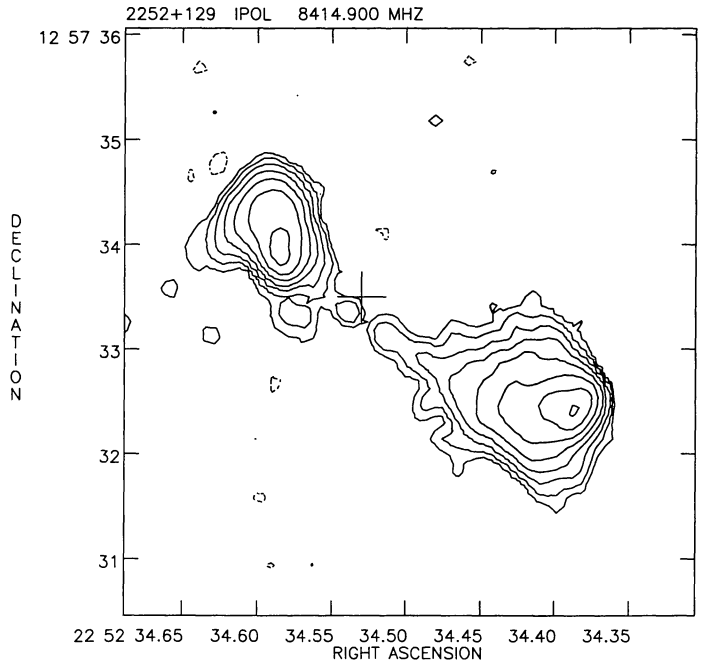

Fig. 51.

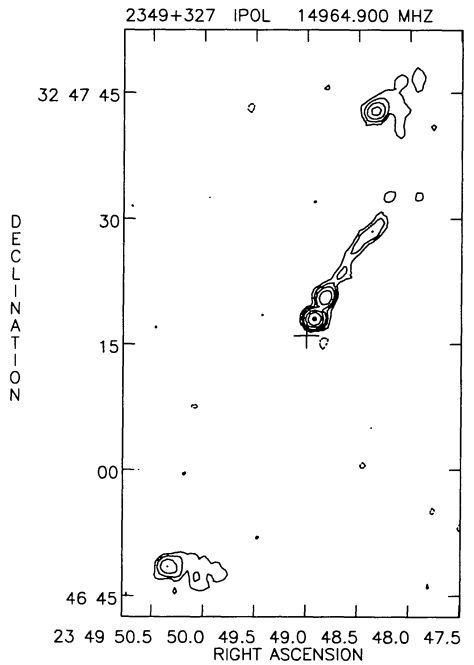

Fig. 52.